Investigating the role of TDP43 dysregulation in driving neuronal degeneration in Amyotrophic Lateral Sclerosis

Submitted by Jessica Board to the University of Exeter as a thesis for the degree of *Masters by Research* in Medical Studies, September 2022.

Abstract

Amyotrophic Lateral Sclerosis (ALS) is a fatal neurodegenerative condition that causes the loss of motor neurons in the brain and spinal cord. Some ALS cases are familial, but around 90-95% are sporadic and patients usually die within 3-5 years due to paralysis. There is no cure for ALS and the main existing treatment lacks effectiveness, thus new therapies are required. To achieve this, creating a disease model is an effective way to try and uncover potential targets. ALS and other neurodegenerative conditions display dysregulations in a RNA binding protein called TDP43 and are collectively known as TDP43 proteinopathies. In these conditions TDP43 can be mislocalized to the cytoplasm and sparse in the nucleus, where it is normally abundant in healthy individuals. TDP43 is involved in regulating splicing and plays a role in microRNA biogenesis. This study uses a method of TDP43 mislocalization as well as independent knockdown to create a disease model to observe the effects of TDP43 dysregulation in differentiated human neurons. This study shows that TDP43 mislocalization is toxic to cell phenotype and causes microRNA downregulation, while TDP43 knockdown and nuclear absence is what dysregulates splicing. Therefore, these results indicate that TDP43 plays a role in neuron death and ALS pathology and targeting this protein, or its dysregulated miRNAs may be beneficial to develop therapies for ALS and other TDP43 proteinopathies. Hence, future experiments can combine the methods from this study to make an accurate in-vitro model of TDP43 pathology as observed in patients and used to investigate miRNAs, splicing defects and possible new therapeutic targets for TDP43 dysregulation in ALS and other neurodegenerative diseases.

List of Contents

List of Figures and Tables

Table of Abbreviations

ALS	Amyotrophic Lateral Sclerosis
AAV	Adeno Associated Virus
AD	Alzheimer's Disease
CNS	Central Nervous System
CRISPR-Cas9	Clustered regularly interspaced short palindromic repeats and CRISPR-associated protein 9
CDS	Coding sequence
C9ORF72	Human chromosome 9 open reading frame 72
DNA	Deoxyribonucleic acid
DNMT	DNA methyltransferase
DMEM	Dulbecco's Modified Eagle Medium
FBS	Foetal Bovine Serum
FTD	Frontotemporal Dementia
FUS	Fused in sarcoma
GFP	Green Fluorescent Protein
gRNA	Guide RNA
KD	Knockdown
mRNA	Messenger RNA
MiRNA	Micro RNA
MAP2	microtubule associated protein 2
MN	Motor Neuron
MT	Mutant
NMJ	Neuromuscular Junction
NES	Nuclear Export Signal
NLS	Nuclear Localisation Signal
PD	Parkinson's Disease
PBS	Phosphate buffered saline
PDL	Poly-D-Lysine
Pre-miRNA	Precursor miRNA
Pri-miRNA	Primary miRNA
qPCR	Quantitative polymerase chain reaction
RA	Retinoic acid
RNA	Ribonucleic acid
RISC	RNA-induced silencing complex
ShRNA	Short hairpin RNA
SOD1	Superoxide dismutase 1
TDP43	TAR DBA-binding protein 43
TARDBP	TAR DNA Binding Protein
TGF-β	Transforming growth factor beta
UTR	Untranslated Region
WT	Wild type

Introduction

Introduction to ALS

The neurodegenerative condition, amyotrophic lateral sclerosis (ALS), is caused by the progressive loss of motor neurons (MNs) in the brain and spinal cord. The main role of MNs is to convey signals from the brain and spinal cord to the muscle and therefore in ALS the skeletal muscles weaken and atrophy. This eventually leads to death within 3-5 years, usually due to paralysis of the respiratory muscles.(1) Most ALS cases are of unknown cause and are sporadic (90-95%), while around 5-10% have genetic factors and are therefore classed as familial cases.(2) Therefore, genetic mutations, environmental factors and even epigenetics could all promote ALS pathology. At present, there is no cure for this devastating disease, but treatments exist that mildly slow its progression.(3,4) Due to these drugs being only somewhat effective, better treatments are required to improve patient prognosis and quality of life. Gaining new insight on the complex mechanisms behind ALS is essential for the development of such therapies.

There are many gene mutations that have been linked to ALS, with the most common ALS mutations found in the Chromosome 9 Open Reading Frame 72 (*C9ORF72*) gene. Around 50% familial cases have mutations in *C9ORF72* which codes for the C9ORF72 protein; this protein is found in the presynaptic terminal of neurons and is involved in processes such as RNA production and transport.(5) Another gene is free radical scavenging enzyme Superoxide Dismutase-1 (*SOD1*), which forms an important part of the intracellular defence mechanisms utilised by cells to protect themselves against free radicals. Mutant *SOD1* accounts for around 20% of familial cases of ALS.(6) Fused in sarcoma (*FUS*) codes for the FUS protein, which binds to deoxyribonucleic acid (DNA) and regulates transcription. Mutations in *FUS* are the third most common in familial ALS after SOD1 with a prevalence of around 4-5% and can disturb ribonucleic acid (RNA) processing and splicing.(5,7)

Finally, another important gene that plays a role in ALS is *TARDBP.* This gene produces instructions for a nuclear protein called Tar DNA binding protein (TDP43) that is dysregulated in neurodegenerative conditions, including ALS. Mislocalized and misfolded TDP43 forms clumps in the cytoplasm and

interferes with normal MN function.(8) TDP43 is a key protein involved in ALS pathology and although *TARDBP* gene mutations are rare in familial ALS (up to 5%), cytoplasmic mislocalization and aggregation of TDP43 are present in 97% of all ALS cases.(2) Therefore, this protein is investigated in the following study as its pathology is relevant to the majority of ALS cases and the main roles of TDP43 will be outlined below. In summary, several key genes are involved in ALS pathology with most implicated in RNA dysfunction.(4-7)

TDP43 in Neurodegeneration

TAR DNA-binding protein 43 (TDP43) is a nuclear protein that binds both RNA and DNA. It plays a main role in the regulation of RNA processing, inclusive of splicing, messenger RNA (mRNA) transport and the biogenesis of small non-coding, regulatory RNAs called micro-ribonucleic acids (miRNAs).(5) TDP43 is encoded by the *TARDBP* gene and is 414 amino acids in length. TDP43 is known to target thousands of RNAs in mammals and preferentially binds to the 3’ untranslated region (UTR) of RNA.(9) The basic structure of TDP43 is shown in figure 1 and shows that TDP43 contains a nuclear localisation signal (NLS). This signal is recognised by transport proteins during nuclear import, meaning that in healthy cells TDP43 is primarily localised to the nucleus.(10) In many neurodegenerative conditions, including ALS, TDP43 is absent from the nucleus and accumulates in the cytoplasm. Genetic mutations in the *TARDBP* gene are known to contribute to the mislocalization in familial cases of ALS and some sporadic cases.(11) However, mislocalization of TDP43 is observed in almost all sporadic incidences of ALS and it is these that account for around 90% of total cases.(2) Importantly, *TARDBP* is not found to be mutated in the majority of these cases, yet TDP43 dysregulation still occurs. Other neurodegenerative conditions including dementia, Parkinson's disease (PD), Alzheimer's disease (AD) can also show some TDP43 dysregulation and the subset of conditions that display dysregulated phosphorylation, cleavage, ubiquitination and/or nuclear deletion of TDP43 are known as TDP43 proteinopathies.(12) Therefore, any research that investigates the role of TDP43 dysregulation in neurodegeneration will be relevant to not only ALS, but other neurodegenerative conditions also.

Figure 1. Schematic showing the basic structure of TDP43. *TDP43 contains two RNA recognition motifs, RRM1 and RRM2 which bind target RNAs, a nuclear localisation signal (NLS) and a nuclear export signal (NES), both involved in transport of TDP43 in and out of the nucleus. The glycine rich terminus present on TDP43 is involved in the aggregation of TDP43 and therefore is also known as a prion-like domain (PrLD).(9)(Schematic adapted from Tziortzouda et al. 2021, created using biorender.com).*

The accumulation of TDP43 within the cytoplasm can lead to the formation of protein aggregates which are likely to contribute to MN dysfunction and death.(13) TDP43 aggregation is widely studied and the presence of these aggregates in the MN cytoplasm are a key hallmark of ALS. TDP43 exists in both full-length and fragmented form to constitute the aggregates seen in ALS.(14) However, it is still debated if these aggregates are what contribute to MN degeneration and how. TDP43 aggregation is present in both familial and sporadic patients and is said to increase oxidative stress within MNs.(15) It is described how the aggregation may prevent TDP43 returning to the nucleus and thus it is unable to carry out critical nuclear tasks. As well as being aggregated in the cytoplasm and therefore inhibiting its cytoplasmic function also.(14) However it is also shown that mislocalized TDP43 does not always aggregate yet is still toxic to the cells. Therefore aggregation is not essential to cause cytotoxicity, but the accumulation of cytoplasmic TDP43 alone is enough to be detrimental to MNs.(16,17) The effect of TDP43 mislocalization on aggregate formation will be looked at in this study to observe if the accumulation of TDP43 in the cytoplasm is enough to cause these inclusions that are not only observed in ALS, but other neurodegenerative conditions like frontotemporal dementia (FTD) and Alzheimer's Disease (AD).(18)

TDP43 and splicing

TDP43 is required for the regulation of splicing of various target RNAs.(19–21) For example, one target of TDP43 is *STMN2*, a gene the encodes a stathmin phosphoprotein, stathmin 2, involved in microtubule regulation and repair.(21,22) Previous work has shown that the expression of this gene is greatly reduced after TDP43 knockdown and mislocalization in patient-specific

MNs, which correlates with the reduction observed in post-mortem patient spinal cords.(21) The lack of TDP43 in the nucleus causes dysregulated alternative splicing of *STMN2* by including a micro exon which contains a premature stop codon. This leads to a truncated protein being made and consequently microtubule regulation is disturbed.(22,23) Additionally, in vivo investigations demonstrate that mice deficient in *STMN2* display motor defects and fragmentation of the neuromuscular junction (NMJ).(22) Dysregulated splicing due to lack of nuclear TDP43 is also observed in other genes, such as *UNC13A*. This gene has a role in vesicle priming to help maintain competent synaptic vesicle fusion, and is therefore essential for signalling at the NMJ.(23) Truncated stathmin-2 has also been observed in other neurodegenerative conditions, such as FTD, along with TDP43 dysfunction.(24) Again showing the impact of TDP43 dysregulation not just in ALS, but other neurodegenerative conditions as well.

DNA methylation is regulated by TDP43

Another process within gene regulation that may be affected by TDP43 mislocalization is DNA methylation.(25,26) Epigenetic modifications such as this are known to contribute to ALS and may drive MN degeneration.(25,27,28) DNA methylation is an epigenetic mechanism that can permit or restrict access of regulatory molecules to DNA and is known to have profound effects on gene regulation.(29) There are two different types of DNA methylation that can occur, one is known as 5-methylcytosine methylation (5mC) and the other is 5-hydroxymethylcytosine methylation (5hmC). Both involve the methylation of cytosine which is present in the DNA primary sequence.(29) The enzymes responsible for the methylation of cytosine are DNA methyltransferases (DNMTs) which catalyse the transfer of a methyl group during DNA methylation. There are five members of the DNMT family of enzymes, and each has a different function. One gene that has been shown to be dysregulated in ALS, dementia and AD is *DNMT3A*.(27,28,30,31) If *DNMT3A* is overexpressed cells experience increased apoptosis, thus increased DNA methylation is thought to be a driver of MN death in ALS and possibly other neurodegenerative conditions.(27)

It has been shown that many miRNAs are disrupted in ALS and other neurodegenerative conditions.(5,32–34) Some of these miRNAs have roles in regulating key pathways within MNs and will be discussed in more detail later. As mentioned, it is also known that TDP43 plays a part in regulating miRNAs.(35,36) The mislocalization of TDP43 may provide a reason for these disruptions seen in miRNA levels. If found to have a causal link, the mechanisms behind TDP43 mislocalization could be investigated to find potential pathways and therapeutic targets which would be beneficial for both familial and sporadic ALS patients, as well as other neurodegenerative conditions.

TDP43 and microRNAs

MiRNAs are small non-coding RNAs, usually 22 nucleotides long, that can regulate the translation of complementary mRNA.(37) Consequently, miRNAs can downregulate mRNA translation and even cause gene silencing by degrading target mRNA. This degradation is done by the RNA induced silencing complex (RISC) in which the miRNA is loaded. Once loaded onto RISC it guides the complex to the target mRNA, see figure 2.(38) All miRNAs have a distinct seed sequence from nucleotides 2-8 and those with matching or similar seed sequences will target similar genes and pathways.(39) Additionally, a single miRNA can target many different genes and thus miRNAs are thought to play a role in many biological pathways.(40,41) For instance, miRNAs control gene expression that is important in MN maintenance, survival, and functioning. Two key genes implicated in ALS, namely *FUS* and *TARDBP,* play a direct role in miRNA biogenesis. Research has shown that TDP43 is required to produce precursor miRNA by interacting with two important complexes. These are the Drosha complex, present in the nucleus, and the Dicer complex which is present in the cytoplasm, see figure 2 for miRNA biogenesis pathway.(35) Both molecules are needed in the processing of primary miRNA (pri-miRNA) (Drosha) and precursor miRNA (pre-miRNA) (Dicer).(42) Therefore, dysfunctional and dysregulated miRNAs are observed in ALS.(32,43) The mislocalization of TDP-43 may play a role in this dysregulation of important miRNAs and therefore contribute to MN death. This study will model the mislocalization of TDP-43 in-vitro and try to uncover any miRNAs that are dysregulated.

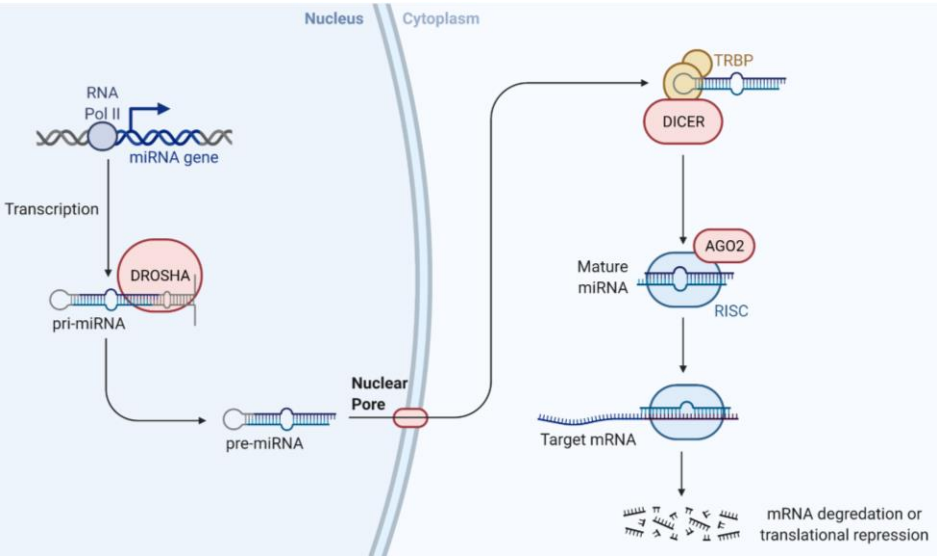

Figure 2. miRNA biogenesis. *miRNA production begins in the nucleus when primary miRNA is transcribed by RNA polymerase and cleaved by Drosha into pre-miRNA. Pre-miRNA is transported into the cytoplasm and cleaved by Dicer. It is unwound into single strands and loaded onto RISC, which degrades the target mRNA and represses translation. Reproduced from Winter et al.(44) (miRNA = micro ribonucleic acid, RNA = Ribonucleic acid, RISC = RNA induced silencing complex).*

The activity of miRNAs can be altered using different methods. To date, clustered regularly interspaced short palindromic repeats and CRISPR associated protein 9 (CRISPR-Cas9) gene editing is a popular method.(45), (46) CRISPR-Cas9 causes the breakage of a specific DNA sequence by using guide RNA (gRNA) to target the enzyme Cas9 nuclease to the desired site, thus allowing complete gene knockout. miRNA knockdown can also be achieved using inhibitors known as “antagomirs”. These are chemically modified antisense oligonucleotides that sequester mature miRNAs, preventing them from binding to their targets, resulting in functional inhibition.(47) A more recent method utilised to achieve miRNA knockdown is known as a miRNA sponge. miRNA sponges are transgenes that can have several target sites to sequester miRNAs.(48)

Many miRNAs have been found to be dysregulated in both sporadic and familial ALS patients.(33,49–51) These include miRNAs such as miR-218, miR-9, miR-139 and miR-7, while other miRNAs such as miR-10a have been shown to be dysregulated in other neurodegenerative conditions such as PD.(52) Several of these miRNAs are also involved in and dysregulated in many cancers.(53–56) As mentioned previously, miRNAs regulate gene expression by targeting and

thus causing the degradation of mRNA. This can silence or inhibit certain genes and has a major impact on biological pathways. miRNAs have been linked to key processes within cells such as the Wnt signalling pathway, the TGF-β/SMAD pathway and other processes such as DNA methylation as mentioned previously.(57–59) Two major pathways that are regulated by miRNAs and play a role in a multitude of diseases are the Wnt signalling pathway and the TGF-β/SMAD signalling cascade.

The Wnt signalling pathway and TGF-β/SMAD signalling pathway. The 'Wnt' pathway is one of the most important signalling cascades that is involved in cell proliferation, differentiation and survival.(60) Dysfunctions that occur within this pathway can be detrimental and consequently Wnt signalling has been linked to many diseases, including cancer, Alzheimer's and ALS.(58,60,61) There are several factors involved within Wnt signalling, with the most widely studied being the canonical pathway, involving β-Catenin.(60) The key steps of this pathway are outlined below in figure 3A. Additionally, The TGF-β/SMAD pathway is involved in multiple cellular processes, inclusive of controlling proliferation, differentiation, apoptosis, migration, immune functions and tumour metastasis.(63) The TGF-β/SMAD pathway has also been implicated in many diseases, such as cancer, fibrosis and neurodegenerative conditions like AD, PD and ALS.(63–68) Targeting this pathway could be promising for future drug discovery for a multitude of pathologies.(63) The key steps of this pathway are illustrated in Figure 3B. Both the Wnt and TGF-β/SMAD signalling pathways, as well as other mechanisms will be looked at during this study to investigate targets of any miRNAs dysregulated following TDP43 mislocalization.

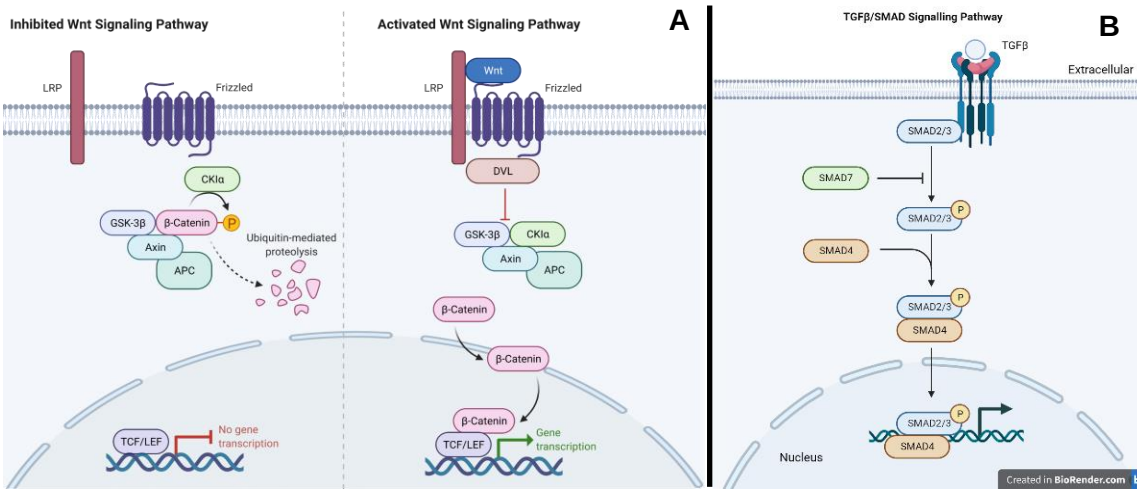

Figure 3. The Wnt and TGF-β/SMAD Pathways. A. The canonical Wnt signalling pathway. *In cells not exposed to the Wnt signal (left panel), β-catenin is degraded by the β-catenin destruction complex (Axin, Adenomatous polyposis coli (APC) and glycogen synthase kinase (GSK-3)). Therefore, it is unable to travel into the nucleus and activate transcription factors T-cell factor/lymphoid enhancer factor (TCF/LEF) and gene transcription does not occur. In the presence of Wnt binding proteins (right panel) Dishevelled (DVL) recruitment by Frizzled (Fz) leads to low-density lipoprotein receptor-related protein 5 or 6(LRP5/6) phosphorylation and Axin recruitment. This disrupts the destruction complex from breaking down β -catenin. Allowing it to accumulate in the nucleus where it co-activates TCF/LEF and gene transcription occurs.(61) Diagram adapted from Hawkins et al.(62)* ***B. The TGF-β/SMAD Signalling pathway.*** *The pathway begins with a transforming growth factor (TGF-β) ligand binding to a SMAD receptor. This causes phosphorylation of the SMAD proteins which enables them to translocate to the nucleus and regulate different transcription factors.(64) Adapted from Burks and Cohn, 2011 (64). Created using Biorender.com.*

Study Aims and Hypothesis

The main aim of this study is to develop an in-vitro model of TDP43 mislocalization and observe the phenotypic changes that occur in neurons. A knockdown model of TDP43 will also be developed and tested to determine whether mislocalization or knockdown of TDP43 is more toxic to neurons, as both are observed in ALS patients. (2,8-12)

A key hypothesis of this project is that TDP43 mislocalization leads to neuronal dysfunction and death by inhibiting neuronal microRNAs. I will deploy the TDP43 mislocalization model to investigate defects in neuronal survival and structure. Further, I will also investigate which miRNAs are dysregulated due to TDP43 mislocalization and potential pathways these are involved in.

Methods

General plastic ware and chemical reagents. Cells were cultured in sterile tissue culture flasks, size T25 (Greiner, UK). Experiments were performed in sterile 96 or 24-well plates (Greiner, UK). Cell suspensions and tissue culture reagents were handled in sterile tubes and aspirated/transferred with serological pipettes.

Cell lines. The cell line SH-SY5Y, neuroblastoma cells from Sigma Aldrich, UK were used and cultured in Dulbecco's Modified Eagle's Medium (DMEM) high glucose (4.50 g/L) (Sigma Aldrich, UK) with L-glutamine, non-essential amino acids and 10% foetal bovine serum (FBS). Cells were differentiated as stated below. Four biological replicates were used, each with two technical replicates.

Cell culture conditions and general practice. All cells and experiments were cultured or incubated at 37°C, 5% CO2 and under atmospheric levels of O2, with a humidified environment. Cells were passaged once 90% confluency was achieved. Passage of SH-SY5Y cells consisted of removal of culture media, brief wash with phosphate buffered saline (PBS), trypsinisation, neutralisation with DMEM media (4.50 g/L glucose) containing 10% FBS centrifugation (1200rpm, 5-minutes) and transfer to a new flask. The cells were counted and resuspended in fresh SH-SY5Y media so the final cell density was ~200,000 cells/ml.

SH-SY5Y differentiation. Plates were coated with 0.01% poly-d-lysine (PDL) overnight and washed twice with PBS. SH-SY5Y cells were then plated as normal in SH-SY5Y media. 24-hours later the media was changed to N2B27 media, consisting of DMEM F12 (glucose 3.15 g/L) containing 10% FBS, 1% N2 and 2% B27 supplements (All purchased from Thermo Fisher, UK) with retinoic acid (RA) at a final concentration of 10 µM. Media was changed to this differentiation media every three days until cells were harvested.

The TDP43 mislocalization model in Differentiated SH-SY5Y Cells. SH-SY5Y cells were plated at a density of 20,000cells/well in black 96-well plates (Perkin Elmer, UK) and at a density of 50,000 cells/well in clear 12-well plates (GreinerBio, UK). Cells were differentiated for 1-week using the differentiation protocol described above. After one week, adeno associated viruses (AAVs)

were added to mislocalize TDP43. All viral preparations and cloning were done by Dr Seema Namboori according to Takara protocol (https://www.takarabio.com/products/gene-function/viral-transduction/adeno-associated-virus-(aav)/packaging-systems-and-cells) and using Takara AAVpro® Extraction Solution (cat #6235). The volume of virus to add was determined empirically, in this case final concentrations decided for all viruses were 0.4 µL per 10,000 cells. Conditions were 0 (control nanobody), M (nanobody with strong NES), TDP43+0 (TDP43-eGFP and control nanobody), TDP43+M (TDP43-eGFP and nanobody with strong NES). 0 and M were included to observe if the nanobody alone had any effect and could also act as controls alongside the control for the TDP-43 overexpression when looking at mislocalization effects. The day after transduction of the AAVs a media change occurred and then every 3 days until day 14 when cells were harvested. Three biological replicates were performed for each condition, (n=3). Immunostaining was carried out as per immunostaining timings and protocol described later. With primary antibodies Rb TDP43 (1:800, cat #10782-2-AP, ProteinTech), Mouse (Ms) TUJ1 (1:1000, cat #MMS-435P-100, BioLegend), Rb caspase 3 (1:400, cat #9664L, Cell Signalling Technologies) and Chicken (Ck) MAP2 (1:16,000, cat #GTX82661, GeneTex). Secondary antibodies were goat anti-Rb (#ab150083), goat anti-Ck (#ab150176), donkey anti-Ms (#ab150105) and donkey anti-goat (#ab150129), all were added 1:2000 (Abcam, UK).

β-Catenin Overexpression. SH-SY5Y cells were plated at a density of 20,000 cells/well in black 96-well plates (Perkin Elmer, UK). Cells were differentiated for one week using the differentiation protocol. After one-week cells were transfected via manufacturers instruction (NeuroMag Transfection, OZ Biosciences, USA) with overexpression plasmid for β-Catenin (CMV-AAV-β-Cat-eGFP) and a GFP control (CMV-AAV-eGFP), both at a final concentration of 400 ng/20,000 cells. Cells were cultured normally for one week and then fixed at day 14 for imaging. Immunostaining protocol was carried out as described below, using primary rabbit (Rb) antibody caspase 3 (1:400, cat #9664L, Cell Signalling Technologies) and secondary goat anti-Rb antibody (1:2000, cat #ab150083, Abcam). Only one biological replicate was performed, n=1.

DNMT3A UTR Transfection. SH-SY5Y cells were plated in white 96-well plates (Thermo Fisher, UK) with a density of 10,000 cells/well in 100 µL media. SH-SY5Y cells were transfected with two plasmids containing the sequence for *DNMT3A*. A concentration of 10 ng/10,000 cells was used for the DNMT3A UTR plasmids and co-transfected with a plasmid containing RFP to check transfection efficiency at a final concentration of 100ng/10,000 cells. The control plasmid contained an unaltered wild-type (WT) sequence for *DNMT3A*. The second plasmid contained mutations (MT) in the 3'UTR target site for miR-218. This was done by the Bhinge lab by mutating bases in the 3' UTR of DNMT3A that corresponded to positions 2, 4, and 6 within the miR-218 seed sequence. Therefore, in the mutated version, miR-218 is unable to bind to the UTR of the *DNMT3A*. The plasmid for *DNMT3A* is a PSI-check plasmid as outlined below, therefore the levels of *DNMT3A* correlated directly with Renilla reading. Three biological replicates were performed, (n=3).

miR-218 Sponge Knockdown and Overexpression Transfection. For luciferase assay: SH-SY5Y cells were plated in white 96-well plates (Thermo Fisher, UK) with a density of 10,000 cells/well in 100 µL media. miR-218 was perturbed using independent methods to both knockdown and cause overexpression of the miRNA. The knockdown plasmid and consists of a miRNA sponge which sequesters miRNAs, and the overexpression plasmid was made by cloning the miR-218 hairpin downstream of the H1 promoter in an AAV plasmid (pAAV-cmv-gfp-h1-mir218, see Figure 1 in appendices for plasmid map). Both were made by Dr Sophie Hawkins prior to this project start. Referring to figure 2, the shRNA overexpression plasmid enters the cells by transfection and are processed by DICER which cuts the precursor miRNA-218 hairpin and thus forms the full length double stranded miRNA-218 allowing its overexpression. These were transfected alongside the miR-218 PSI-check plasmid. All plasmids were used at a final concentration of 100 ng/10,000 cells, with a concentration of 10 ng/10,000 cells for the PSI-check plasmid. After 72-hours a luciferase assay was carried out. One biological replicate was performed, (n=1).

For immunostaining: SH-SY5Y cells were plated in black 96-well plates (Perkin Elmer, USA) at a larger density of 50,000 cells/well in 100 µL media. All plasmids were used at a final concentration of 100 ng/10,000 cells. The controls

were an empty sponge control for the miR-218 sponge, and an OCT4 shRNA control for the miR-218 overexpression. Puromycin was added at a final concentration of 1 µ/mL in the media changes post-transfection to kill cells that had not been transfected, as both the knockdown and overexpression plasmids used are all puromycin resistant. After 72-hours cells were fixed and immunostaining carried out. Immunostaining protocol was carried out as described below, using primary Rb antibody DNMT3A at 1:1000 (cat #GTX129125, Genetex, USA) and secondary goat anti-Rb antibody 1:2000 (cat #ab150083, Abcam, UK). Three biological replicates were performed, (n=3).

PSI-check reporter system. PSI-check vectors were purchased from Promega, UK and edited by the Bhinge lab for use. The PSI-check vectors were used as a reporter system to help quantify the amounts of endogenous target miRNA or mRNA in the cells following transfections (figure 4). Two vectors will be used, one with the target mRNA or miRNA binding site and one without.

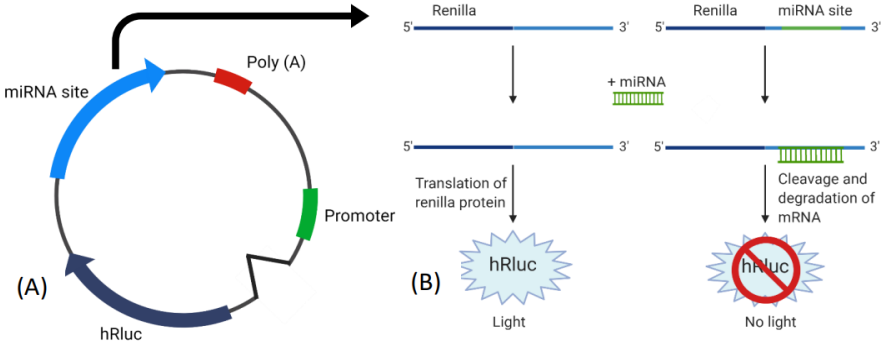

Figure 4. Schematic diagram of PSI-check reporter system. *Two PSI-check vectors were used, one with a binding site for the target miRNA and one with no binding site. (A) A PSI-check with the miRNA binding site. (B) How the reporter system works. The left side depicts either the PSI-check with no miRNA binding site or what happens if the target miRNA has been sequestered. The right shows the PSI-check with the miRNA binding site; the miRNA cleaves the renilla luciferase mRNA. (miRNA = micro ribonucleic acid, mRNA = messenger ribonucleic acid). Created with BioRender.com.*

shRNA synthesis for knockdown of TDP43. Short hairpin RNAs (shRNAs) were designed to target the sequence for the *TARDBP* gene responsible for TDP43 production. Three were made, two that target the coding sequence and one that targeted the 3'UTR of *TARDBP* (Table 1 in the appendices for primer sequences). These were transfected into a lentivirus using envelope plasmid pMD2.G (Addgene, USA, #12259) and packaging plasmid pspax2 (Addgene, USA, #12260). The virus was synthesised in 293FT cells and cultured with 500

µL/mL Geneticin (G418) (Thermo Fisher Scientific, UK). Media that contained the virus was collected and titrated to determine an efficient viral volume needed in future experiments.

shRNA Transduction in Differentiated SH-SY5Y Cells. SH-SY5Y cells were plated at 20,000 cells/well in black 96-well plates and differentiated for one week. After which they were transduced with the shRNA lentiviruses added at final concentration of 2 µL/10,000 cells. As a control, an shRNA targeting the Renilla gene was used, which is not expressed in SH-SY5Y cells. They were cultured as normal and on day 14 fixed for immunostaining protocol which was carried out as below. The same antibodies were used as before following the nanobody model, these were primary antibodies Rb TDP43 (1:800, cat #10782-2-AP, ProteinTech), Mouse (Ms) TUJ1 (1:1000, cat #MMS-435P-100, BioLegend), Rb caspase 3 (1:400, cat #9664L, Cell Signalling Technologies) and Chicken (Ck) MAP2 (1:16,000, cat #GTX82661, GeneTex). Secondary antibodies were goat anti-Rb (#ab150083), goat anti-Ck (#ab150176), donkey anti-Ms (#ab150105) and donkey anti-goat (#ab150129) added 1:2000 (Abcam, UK).

Immunostaining*.* After treatments, cells were fixed with 4% paraformaldehyde (PFA) (Sigma, United States), permeabilized with 100% methanol (MeOH) and blocked in PBS (+$MgCl_2$, +$CaCl_2$) containing 1% BSA for 1 hour at room temperature (RT). Cells were stained with primary antibodies in 1% BSA at 4°C overnight. The following day, after three washes with PBS, the cells were further incubated with a secondary antibody (1:2000, Abcam) in 1% BSA for 1-2 hours at RT. Simultaneously, in all immunostaining performed, nuclei were stained using Hoechst dye (1:1000). See Table 2 in the appendices for collated list of antibodies used. Images were viewed and acquired using the ImageXpress PICO microscope software (USA). Images created using ImageJ software, cell fluorescence intensity was quantified using Cell Profiler software or by using the ImageXpress PICO analysis software.

Quantitative real-time PCR. Total RNA was isolated using the monarch total RNA miniprep kit (New England Biolabs, UK) as per manufacturer's instructions and reverse transcribed to cDNA using Mir-X™ miRNA First Strand Synthesis K

(Takara Bio, USA) for miRNA analysis and High-Capacity cDNA Reverse Transcription Kit (Thermofisher, UK) for mRNA analysis. Quantitative real-time PCR was performed using SYBR Green qPCR Master Mix (Thermo Fisher Scientific) on a Quantstudio-6 Real-Time PCR system (Thermofisher, UK). miRNA expression from qPCR is represented as gene expression relative to *RNU5, RNU6 and HPRT1* housekeeping genes. mRNA expression was relative to *HPRT1, GAPDH, ACTB, TBP* and *RPL13* housekeeping genes. Sequences were obtained from Origene.com and oligonucleotides ordered from Integrated DNA Technologies (IDT, USA). The delta-delta Ct ($2^{-\Delta\Delta Ct}$) method was used to analyse the qPCR data and calculate the relative fold gene expression.

Dual Luciferase assay. The Dual-Glo Luciferase Assay System was used to quantify miRNA and was carried out to the manufacturer's instructions (Promega, uk). The PSI-check vector was used as a reporter system.

***Biological replication*.** For all assays, a minimum of three independent experiments were performed (n=3), each containing two technical replicates, and appropriate statistics carried out unless stated otherwise.

Statistical testing. Data are presented as the average ± standard error (SE), as SE shows the variability of the sample average from the population average. All graphs were made, and statistical tests conducted using Excel or GraphPad (USA) unless stated otherwise in legends. One-tailed, unpaired t-tests were used to look for any statistically significant differences between control and treatment groups. A *P*-value ≤ 0.05 was considered significant.

Results

Optimisation of a model to mislocalize TDP43 in differentiated SH-SY5Y cells

A nanobody model to mislocalize TDP-43. A model was optimised to overexpress TDP43 in differentiated SH-SY5Y cells and then mislocalize this TDP43 into the cytoplasm. This was to mimic what is observed in ALS and other TDP43 proteinopathies. Firstly, neuroblastoma cells were successfully differentiated following a 2-week protocol that utilises retinoic acid (RA), see figure 5A. Images showing the final network stained for primary neuronal markers TUJ1 and MAP2 in figure 5B. To mimic TDP43 mislocalization in SH-SY5Y cells an overexpression model was optimised using two AAVs. One of these consisted of a TDP43-GFP-AAV construct that increased levels of TDP43 in the cells; this induced TDP43 would have a green fluorescent protein (GFP) tagged to it. The second AAV was synthesised, by the Bhinge lab, to include an anti-GFP construct. This construct is known as a nanobody and binds to a small portion of the GFP. The nanobody is also tagged to a strong nuclear export signal (NES) taken from the MAPK gene, thus known as NESM in the following study. The strong NES therefore overrides the NLS on the overexpressed TDP43 and therefore prevents it from being shuttled back into the nucleus, causing it to mislocalize to the cytoplasm. The control was an anti-GFP construct with no NES, thus no mislocalization would occur (NES0), see figure 5C below.

The model successfully mislocalized overexpressed TDP43 from the nucleus to the cytoplasm. This mislocalization can be seen in the immunofluorescent images below where TDP43-GFP is stained as green, see figure 5D. The images show that in the control (T+0) overexpressed TDP43 is mainly nuclear, whereas in the cell treated with the nanobody (T+M) the TDP43 is present in the cytoplasm. The box and whisker plot in figure 5E shows the ratio of nuclear TDP43 to cytoplasmic TDP43 (N/C) for all replicates (n=3), thus the more nuclear TDP43, the bigger the reading. T+M had a significantly higher cytoplasmic TDP43 ratio compared to the T+0 control ($P \leq 0.01$), indicating that the model can cause mislocalization of overexpressed TDP43 in differentiated SH-SY5Y cells.

Figure 5.

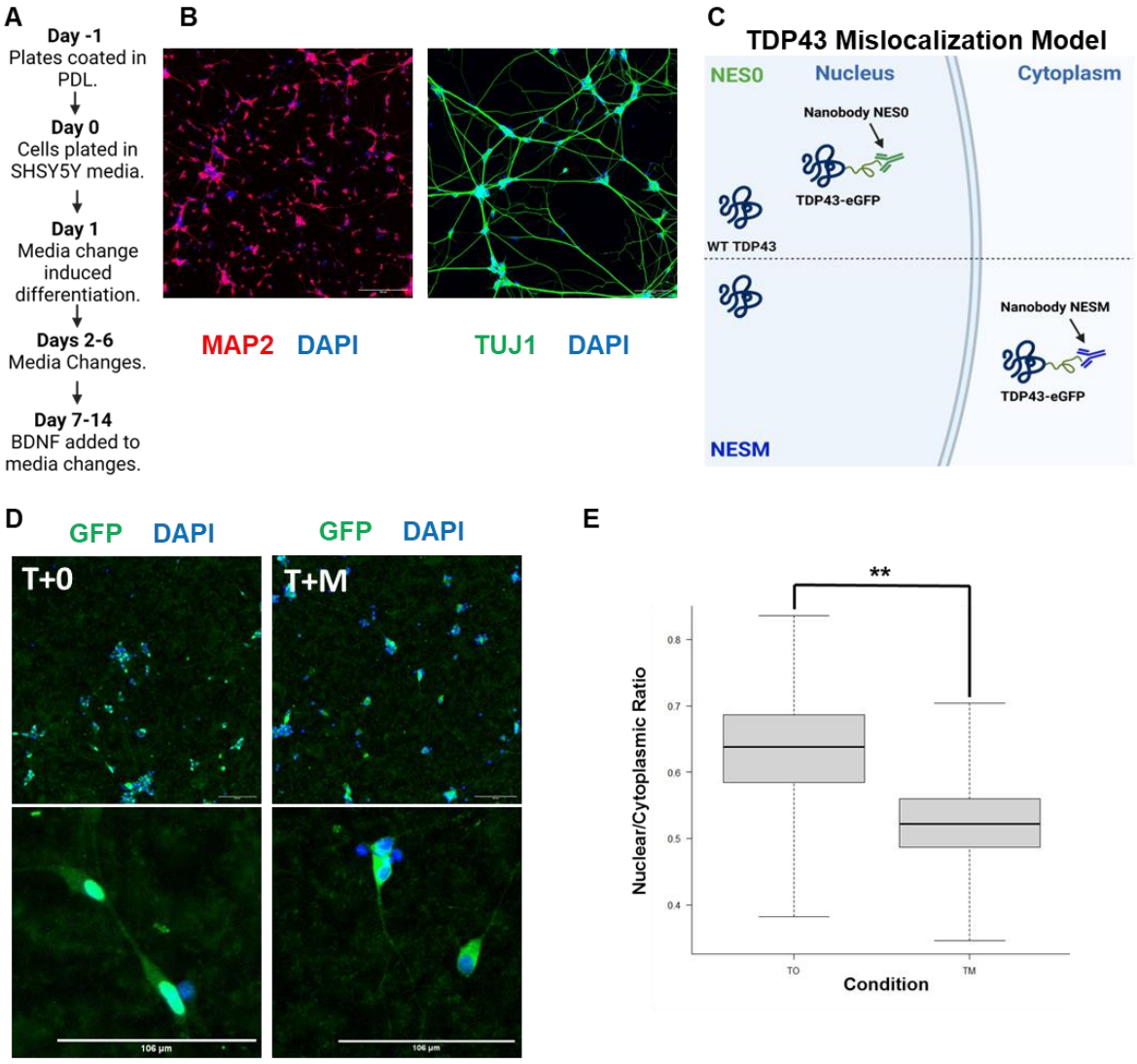
A
Day -1
Plates coated in PDL.
Day 0
Cells plated in SHSY5Y media.
Day 1
Media change induced differentiation.
Days 2-6
Media Changes.
Day 7-14
BDNF added to media changes.
B
MAP2 DAPI
TUJ1 DAPI
C
TDP43 Mislocalization Model
NES0
Nucleus
Cytoplasm
Nanobody NES0
TDP43-eGFP
WT TDP43
Nanobody NESM
TDP43-eGFP
NESM
D
GFP DAPI
GFP DAPI
T+0
T+M
106 µm
106 µm
E
**
Nuclear/Cytoplasmic Ratio
0.8
0.7
0.6
0.5
0.4
TO
TM
Condition

Figure 5. A TDP43 mislocalization model.

(A) Schematic representation of the 2-week RA protocol used to differentiate SH-SY5Y cells. Created with BioRender.com.

(B) Images to show SH-SY5Y cells successfully express neuronal markers following 2-week differentiation using RA. Staining with Hoechst nuclear dye (blue) and neuronal markers MAP2 (red) and TUJ1 (green), scale is 106um.

(C) Schematic of the TDP43 mislocalization model. TDP43-GFP is overexpressed in cells, with the nanobodies having antiGFP sequences that recognise and bind to the GFP on the transduced TDP43. The NESM has a strong NES signal which overrides the pre-existing NLS and TDP43-GFP remains in the cytoplasm. Control nanobody is NES0 where no NES signal is present, therefore transduced TDP-43-GFP is shuttled back into the nucleus due to the NLS.

(D) Differentiated SH-SY5Y cells show TDP43-GFP mislocalized to the cytoplasm. Images show T+0 (control nanobody) (left) and T+M (NES nanobody) (right) with TDP43-GFP (green) being mainly nuclear for the control and mislocalization to the cytoplasm following use of the NESM nanobody. Nuclear stain is Hoechst (blue), scale is 106um.

*(E)The box and whisker plots show the distribution inclusive of minimum, maximum and median N/C TDP43 ratio values across all replicates, n=3. A two sample t-test was performed assuming equal variance. P-values ≤ 0.05 were considered statistically significant, **P ≤ 0.01. Graph and statistics done in R.*

Differentiated SH-SY5Y cells show a cell and molecular phenotype following TDP43 mislocalization

Neuronal death is increased in neurodegenerative conditions; therefore, caspase activity was investigated to see if TDP43 mislocalization increases apoptosis in differentiated SH-SY5Y neurons. Following successful mislocalization of TDP43, caspase intensity was analysed following immunofluorescent staining. Figure 6A and B show that caspase activity is increased following mislocalization of TDP43, as in comparison to the control group there was around a 30% increase in average caspase activity. Following statistical analysis using a t-test this increase is seen to be significant across the whole sample ($P \leq 0.01$) as well as between averages ($P=0.0055$). To make sure the NESM nanobody alone did not affect caspase activity, the 0 and M groups were also compared (6C and D). A small, significant decrease in caspase is observed between the NES0 and NESM group across all cells ($P \leq 0.01$). However, the variance between conditions was low and thus when comparing the averages for each group, it showed no significant difference ($P=0.21$). Therefore, the NESM is unlikely to affect caspase activity on its own, and the mislocalization of TDP43 significantly increases caspase activity in differentiated SH-SY5Y neuronal cells.

The neuronal network was also analysed using the marker TUJ1, which stains the cell bodies, dendrites, axons, and neurite branches of neurons and therefore can be used to analyse the neuronal network. This is as diseased neurons display shorter axons and less branching and it could be investigated if TDP43 mislocalization contributes to this disease phenotype. Firstly, figures 6E and F show that the nanobody has no significant effect on branching and outgrowth in differentiated SH-SY5Y cells. There was a slight, non-significant, increase in branching and outgrowth for the T+0 condition, where overexpressed TDP43 is present in the nucleus. However, when the NESM nanobody is introduced and mislocalization of TDP43 occurs, there is a decreased trend in both neurite outgrowth and branching. A representative image of the neuron network stained with TUJ1 (green) for T+0 and T+M can be seen in figure 6G. Although the change observed is not significant, the

decreased trend is what is expected following mislocalization of TDP43 in neurons.

Additionally, TDP43 dysregulation has also been shown to affect the proteins STMN2 and UNC13A that are involved in synapse and microtubule maintenance. It is known that these genes undergo splicing defects when TDP43 is depleted which causes the inclusion of a cryptic exon in the *UNC13A* and *STMN2* genes. This results in the UNC13A protein not being produced and a truncated version of the STMN2 protein being made. Therefore, qPCR was used to measure the normal genes, the truncated version for *STMN2* (TRUNC) and the *UNC13A* transcript containing the cryptic exon (CE). The results can be seen in figure 6H and show that there is no significant change following mislocalization of TDP43 on *STMN2* (P=0.33) and its truncated version (P=0.08), whereas a small significant decrease can be observed for *UNC13A* (P=0.03). It is expected that the *STMN2* (TRUNC) would be increased, and the healthy gene decrease, as well as an increase in the *UNC13A (CE)*. Interestingly however, *UNC13A* (CE) was undetectable and therefore not being expressed following mislocalization. Therefore, the data confirms that the normal genes are still being expressed, with the truncated or altered versions barely affected. As a result, TDP43 mislocalization via this mislocalization model is not enough to alter these genes as dramatically as what is observed in patients. This is likely due to the WT TDP43 still being present in the nucleus of the neurons, and therefore would need to be repeated using a model were nuclear TDP43 is ablated as this is more relevant to patients.

Figure 6.

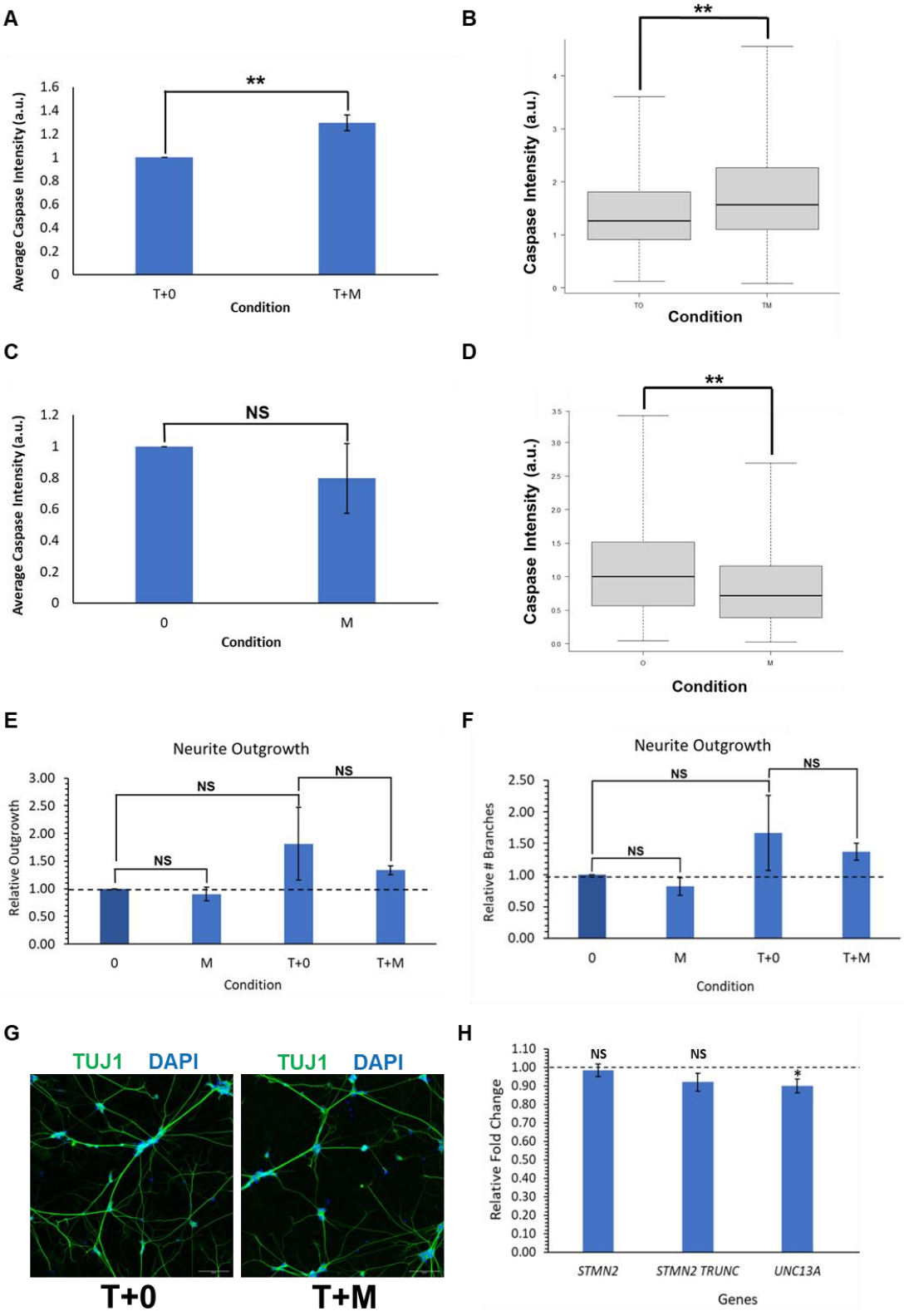
A
Average Caspase Intensity (a.u.)
**
T+0
T+M
Condition
B
Caspase Intensity (a.u.)
**
TO
TM
Condition
C
Average Caspase Intensity (a.u.)
NS
0
M
Condition
D
Caspase Intensity (a.u.)
**
O
M
Condition
E
Neurite Outgrowth
Relative Outgrowth
NS
NS
NS
0
M
T+0
T+M
Condition
F
Neurite Outgrowth
Relative # Branches
NS
NS
NS
0
M
T+0
T+M
Condition
G
TUJ1 DAPI
TUJ1 DAPI
T+0
T+M
H
Relative Fold Change
NS
NS
*
STMN2
STMN2 TRUNC
UNC13A
Genes

Figure 6. TDP43 mislocalization causes a disruption in phenotype in differentiated SH-SY5Y cells.

*(A+B) Caspase activity increases following TDP43 mislocalization. A) Bar chart showing average caspase intensity ± standard error (SE) for T+0 and T+M groups. B) Box and whisker plot showing distribution of caspase intensity with median, minimum and maximum values. T-test statistical analysis looking at the whole sample (B) and averages (A) both showed a significant change between T+0 and T+M conditions, n=3, P-values ≤ 0.05 were considered statistically significant, **P ≤ 0.01. For B, graph and statistics done in R.*

*(C+D) Treatment with nanobody alone has no effect on caspase activity. A) Bar chart showing average caspase intensity ± standard error (SE) for 0 and M groups. B) Box and whisker plot showing distribution of caspase intensity with median, minimum and maximum values. T-test statistical analysis showed a significant change between 0 and M on the whole sample, however no significant change was observed between averages, n=3. P-values ≤ 0.05 were considered statistically significant, **P ≤ 0.01, NS=not statistically significant. For D, graph and statistics done in R.*

(E+F) Neurite outgrowth and branching analysis following TDP43 mislocalization. Bar charts show average outgrowth and number of branches per cell normalised to 0 control ± SE. Analysis was carried out using TUJ1 marker and PICO analysis software. 0 vs M, 0 vs T0, and T0 vs TM were statistically analysed using a t-test. P-values ≤ 0.05 were considered statistically significant, NS=not statistically significant.

(G) Representative images showing neuronal networks for T+0 and T+M groups stained using an antibody for TUJ1 (green) and nuclear Hoechst dye (blue). Scale is 106um.

*(H) Gene expression changes for genes linked to synapse and microtubule maintenance following TDP43 mislocalization. All results were normalised to T+0 values, indicated by the dotted line on the graph at 1. Results presented are average fold change compared to control ± standard error (SE). A two-sample t-test was performed assuming equal variance, n=3. P-values ≤ 0.05 were considered statistically significant, *P ≤ 0.05, **P ≤ 0.01, NS=not statistically significant.*

miRNAs become dysregulated following TDP43 mislocalization

Differentiated SH-SY5Y cells show changes in miRNA gene expression following TDP43 mislocalization. SH-SY5Y cells were differentiated and transduced using the TDP43 model as described previously. A selection of miRNAs were chosen based on previous bioinformatic analysis performed by the Bhinge lab that looked at altered miRNAs in sporadic cases of ALS. These miRNAs were screened using qPCR to observe if they are expressed/altered in differentiated SH-SY5Y cells upon treatment. Figure 7A below shows the gene expression for different miRNAs tested normalised to the control (T+0), with housekeeping genes *HPRT1, RNU5* and *RNU6.* Many of the miRNAs tested showed a significant downregulation in expression following TDP43 mislocalization (miR139: 0.59, *P*=0.0042) (miR-10a: 0.52, *P*=0.0013) (miR-9-3p: 0.45, *P*=0.0038) (miR-9-5p: 0.61, *P*=0.011) (miR-29a: 0.46, *P*=0.0050). However, miR-342 and miR-218 did not give a significant result.

Although miR-218 was not significant, it still showed a decrease in relative expression compared to the control (0.68, *P*=0.064). The downregulation observed may have increased if the experiment ran for an extended period as AAVs can take longer to be expressed in cells. Therefore, it was decided to not ignore the decrease seen in miR-218, although non-significant. Additionally, the CT values observed for miR-9-3p and miR-342 were much higher compared to the other miRNAs tested (CT>31). Therefore, there was less detectable target RNA for this sample, leaving the results unreliable and these were omitted from future investigation. Several of these miRNAs are known to be involved in different cell signalling pathways, so qPCR analysis was performed to observe any expression changes in genes from key pathways implicated in neurodegenerative disease.

Differentiated SH-SY5Y cells show changes in gene expression following TDP43 mislocalization. Previous work from the Bhinge lab has shown that miR-139 can target the WNT pathway in MNs.(62) Additionally, several miRNAs can target the TGF-β pathway, like miR-10a.(69–71) Hence, we investigated whether the WNT and TGF-β pathways were upregulated after TDP43 mislocalization. Figure 7B shows the gene expression changes for these genes with fold changes normalised to the controls (±SE). Housekeeping genes were *GAPDH, HPRT1, TBP, ACTB* and *RPL13. WNT3A, WNT7A, WNT10B* and *ITGA5* showed upregulation in expression. Whereas *WNT4, WNT11* and *CCND3* indicate some downregulation following TDP43 mislocalization. All other genes tested did not indicate a change in gene expression following TDP43 mislocalization. Due to large biological variation, the changes observed were not statistically significant, other than the small downregulation seen in a cancer related gene *CCND3,* which is involved in the cell cycle (0.9, *P*=0.037). Although the changes have not shown statistical significance, the overall trend for some of the genes were prominent. Such as *ITGA5* (2.71), *WNT3A* (3.24), *WNT7A* (2.08), *WNT10B* (1.57), *WNT4* (0.86), *WNT11* (0.89), *TGF-βI* (0.90). As the Wnt genes were the ones that seemed to show the most changes in gene expression, miR-139 and miR-218 were the main focus of the following experiments as they have not only been shown to be downregulated in patients but are known to be involved in regulating this pathway.

Figure 7.

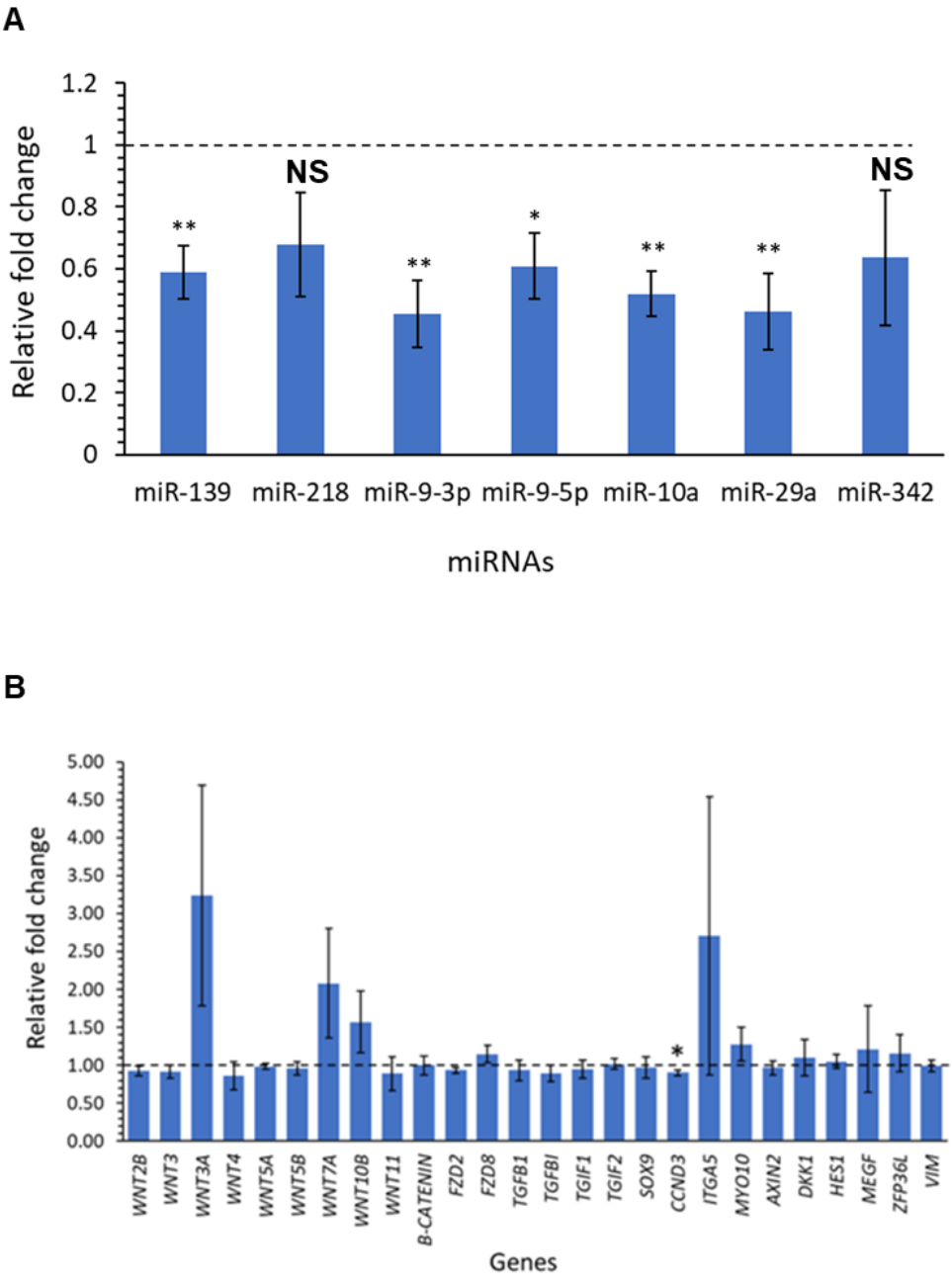
A
Relative fold change
1.2
1
0.8
0.6
0.4
0.2
0
NS
NS
**
**
*
**
**
miR-139
miR-218
miR-9-3p
miR-9-5p
miR-10a
miR-29a
miR-342
miRNAs
B
Relative fold change
5.00
4.50
4.00
3.50
3.00
2.50
2.00
1.50
1.00
0.50
0.00
*
WNT2B
WNT3
WNT3A
WNT4
WNT5A
WNT5B
WNT7A
WNT10B
WNT11
B-CATENIN
FZD2
FZD8
TGFB1
TGFBI
TGIF1
TGIF2
SOX9
CCND3
ITGA5
MYO10
AXIN2
DKK1
HES1
MEGF
ZFP36L
VIM
Genes

Figure 7. miRNA and related pathway gene expression following TDP43 mislocalization.

*(A) miRNA gene expression changes following TDP43 mislocalization. miRNA levels were measured in the mislocalized (T+M) group and normalised to the control, nuclear TDP43 group (T+0) indicated by the dotted line on the graph at 1. Results presented are relative average fold change compared to control ± SE. A t-test was performed assuming equal variance, n=3, P-values ≤ 0.05 were considered statistically significant, *P ≤ 0.05, **P ≤ 0.01, NS = not statistically significant.*

*(B). Gene expression changes for genes involved in key cellular pathways following TDP43 mislocalization. All results were normalised to T+0 values indicated by the dotted line at 1. Results presented are relative average fold change compared to control ± SE. A two-sample t-test was performed, n=3. P-values ≤ 0.05 were considered statistically significant, only one gene (CCND3) showed a significant result, *P ≤ 0.05, while the rest of the genes tested showed no statistically significant change in expression.*

Downstream targets of miRNAs dysregulated following TDP43 mislocalization

miR-218 targets DNA methylation enzyme DNMT3A. miR-218 is known to be the most down regulated miRNA in ALS and in this study qPCR miRNA analysis showed it was downregulated following mislocalization of TDP43. By using a program called Target Scan that shows targets of miRNAs, the gene for methylation enzyme DNMT3A was discovered to have a target for miR-218 in its 3'UTR. SH-SY5Y cells were transfected with two plasmids containing the sequence for *DNMT3A*. The control plasmid contained an unaltered sequence in the UTR of *DNMT3A*, whereas the second plasmid contained a mutated site where the sequence for miR-218 resides. Thus miR-218 would be unable to bind and target the *DNMT3A* mRNA for degradation. The plasmid for *DNMT3A* is a PSI-Check plasmid as mentioned in methods, therefore the levels of *DNMT3A* correlate directly with renilla.

Following independent transfection of these plasmids in SH-SY5Y cells, it can be seen in figure 8A that miR-218 may directly target the UTR of *DNMT3A*. In the WT version, where miR-218 can bind, there is an average *DNMT3A* reading of 2.58. Whereas in the cells that were transfected with the MT DNMT3A plasmid, there is an increase in renilla reading by 0.64 to 3.22. This shows that miR-218 may target and thus regulate *DNMT3A* mRNA expression, however after performing a t-test, the result was non-significant due to some variability between replicates (P=0.28) (n=3). To investigate this further, subsequent overexpression and knockdown experiments were performed on miR-218 to see if *DNMT3A* is altered following miR-218 perturbation using methods to independently knockdown and increase miR-218 levels. A shRNA AAV plasmid was used to cause overexpression of miR-218, while a miR-218 sponge was used to sequester miR-218.

Perturbing miR-218 in SH-SY5Y cells and the effect on DNMT3A. Figure 8B shows a schematic for the basic structure of a miRNA sponge containing three binding sites for a target miRNA. miRNAs bind to these sites and are sequestered, preventing them from binding to their target mRNAs. Therefore, miRNA sponges can be used to investigate miRNA loss-of-function mechanisms. In addition, multiple binding regions on a miRNA sponge allows both short and long-term knockdown. This study utilised a miRNA sponge that has been developed in the Bhinge lab to target miRNA-218. The two plasmids mentioned previously were transfected alongside the PSI-Check plasmids containing the WT and MT versions of the *DNMT3A* UTR miR-218 site. As a positive control, the plasmids were also co-transfected with a PSI-Check plasmid for miR-218 to confirm the knockdown and overexpression had been successful. As seen in figure 8C the miR-218 sponge was able to sequester miR-218 as a 3.5-fold increase can be observed in renilla reading. Additionally, the overexpression plasmid successfully increased the levels of miR-218 as renilla decreased by 1.6. Therefore, these methods can be used to successfully perturb miR-218 in SH-SY5Y cells.

To observe if perturbing miR-218 has any effect on DNA methylation enzyme, DNMT3A, the same transfection was carried out as mentioned above. However, in subsequent media changes puromycin antibiotic was added (final concentration 1ug/ml) to kill any cells that had not been transfected with the puromycin resistant plasmids. An immunostaining protocol was carried out on the remaining transfected cells using a primary antibody for methylation enzyme DNMT3A. Figure 8D shows the average DNMT3A intensity for each condition normalised to the controls. Significant changes were detected following t-test analysis between the empty sponge control and miR-218 sponge (P=0.0015). However, there was no significant change between the OCT4 control and miR-218 overexpression (P=0.26). This can be observed more clearly in figure 8E where the violin plot shows the distribution of the cell intensities for each condition, with the median values indicating there is not an obvious difference between conditions. Therefore, without further investigation, it is shown that miR-218 perturbation only gives a small significant effect on *DNMT3A* expression.

Figure 8.

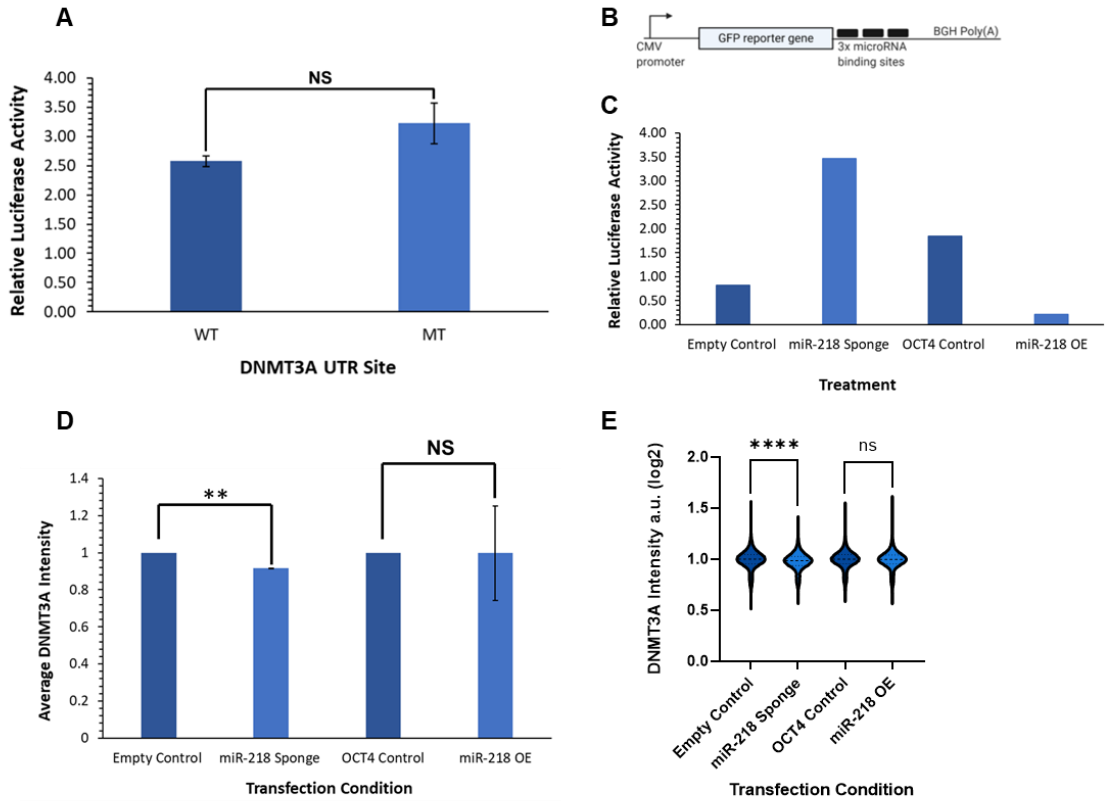
A
Relative Luciferase Activity
4.00
3.50
3.00
2.50
2.00
1.50
1.00
0.50
0.00
NS
WT
MT
DNMT3A UTR Site
B
CMV promoter
GFP reporter gene
3x microRNA binding sites
BGH Poly(A)
C
Relative Luciferase Activity
4.00
3.50
3.00
2.50
2.00
1.50
1.00
0.50
0.00
Empty Control
miR-218 Sponge
OCT4 Control
miR-218 OE
Treatment
D
Average DNMT3A Intensity
1.4
1.2
1
0.8
0.6
0.4
0.2
0
**
NS
Empty Control
miR-218 Sponge
OCT4 Control
miR-218 OE
Transfection Condition
E
DNMT3A Intensity a.u. (log2)
2.0
1.5
1.0
0.5
0.0
****
ns
Empty Control
miR-218 Sponge
OCT4 Control
miR-218 OE
Transfection Condition

Figure 8. miR-218 targets DNA methylation enzyme DNMT3A.

(A). miRNA-218 targets DNMT3A mRNA. Results from dual luciferase reporter assay performed 72-hours post transfection. Graph shows average ± SE, a t-test was performed to analyse differences between groups, n=3, NS = not statistically significant.

(B). Basic structure of a miRNA sponge. A miRNA sponge contains a viral promoter (cytomegalovirus = CMV), reporter gene (green fluorescent protein = GFP), a target sequence for a specific miRNA, and a terminator sequence (bovine growth hormone = BGH). (miRNA = micro ribonucleic acid). Created with BioRender.com.

(C). miR-218 levels can be perturbed in SH-SY5Y cells. Bar graph shows renilla mRNA levels compared to control after treatment with a miR-218 sponge or overexpression plasmid for miR-218. A PSI-Check plasmid was used to determine renilla levels and has a binding site present for miR-218. (Columns 1 and 2) Sponge sequesters miR-218 and thus the PSI-Check plasmid is not targeted and broken down. Renilla reading is higher and thus 'rescued' compared to control. (Columns 3 and 4) Overexpression plasmid increases miR-218 levels, more can target PSI-Check plasmid for degradation, thus Renilla reading is decreased. n=1, thus no statistical testing performed.

*(D). Perturbation of miR-218 is unlikely to affect DNMT3A in SH-SY5Y cells. Bar chart showing average DNMT3A intensity ± SE. T-test analysis was performed to analysis differences between each control and condition, n=3, **P ≤ 0.01, NS = not statistically significant.*

*(E). Violin plot showing the distribution of DNMT3A intensity. Plots show the median, minimum, maximum values of log2 DNMT3A intensities for each treatment. T-test analysis was performed to analyse differences between each control and condition, n=3, ****P ≤ 0.0001, NS = not statistically significant.*

β-Catenin overexpression increases cell death in differentiated SH-SY5Y cells. miR-139 is another miRNA that has been shown to be implicated in ALS, and recently it was linked to the canonical Wnt signalling pathway. It was shown that when downregulated, it causes hyperactivation of canonical Wnt and consequently an increase in β-Catenin. The miRNA qPCR data in this study also showed that following TDP43 mislocalization, miR-139 was significantly downregulated in the differentiated SH-SY5Y cells. Therefore, a transfection was carried out to overexpress β-Catenin in differentiated SH-SY5Y cells. The plasmids used consisted of a shRNA AAV plasmid containing the sequence for β-Catenin with a GFP as a fluorescent marker and the control was an empty plasmid with just the GFP marker present. A preliminary transfection was performed using two concentrations of plasmid, 400ng and 600ng, and after 48 hours caspase intensity was measured using immunostaining.

Figure 9A shows the average caspase intensities for both concentrations normalised to their GFP controls used at the same final concentrations. Only cells that were GFP positive were measured for caspase intensity. Figure 9B shows violin plots of the distribution of the caspase intensities across all cells. There was an 85% increase in caspase activity for the 400ng condition, while a 40% increase can be seen for the 600ng condition. More cell death was observed in the 600ng condition and this was likely due to the large amount of plasmid rather than β-Catenin overexpression alone. Only one replicate was performed (n=1) and therefore no statistics were carried out. β-Catenin transfection efficiency was low due to a large plasmid size of around 3Kb bigger than the control (7Kb). More optimisations need to be carried out to find a more effective transfection method for this plasmid before biological replicates can be performed. However, the overall trend does support the statement that increasing levels of β-Catenin causes an increase in programmed cell death.

Figure 9.

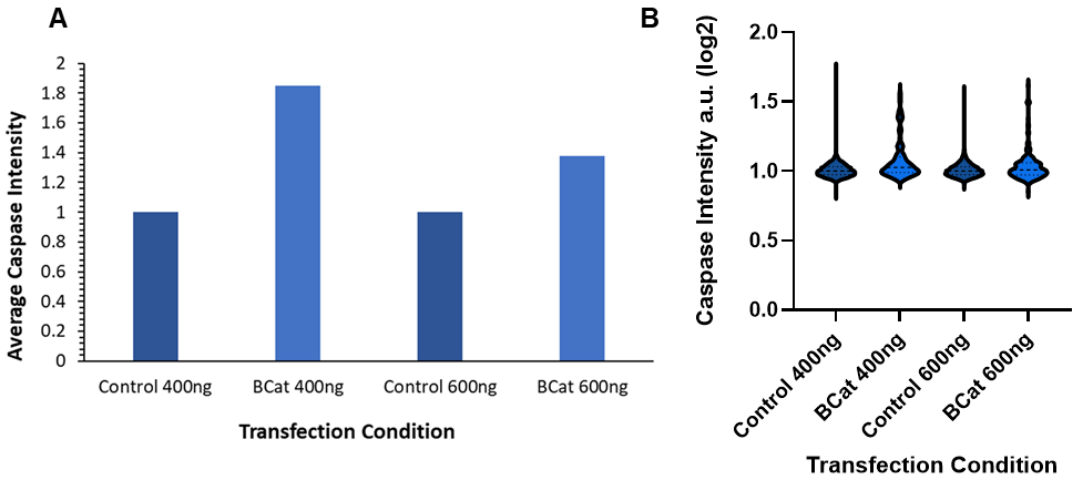

Figure 9. β-Catenin overexpression may increase apoptosis in differentiated SH-SY5Y cells.

(A) Overexpression of β-Catenin may increase caspase activity in differentiated SH-SY5Y cells. Bar chart showing average caspase intensity ± SE for each concentration normalised to respective control, n=1, thus no statistical analysis performed.

(B) Violin plot showing the distribution of caspase intensities following β-Catenin overexpression. Plots show the minimum, maximum and median caspase intensities (log2) for each condition. n=1, thus no statistical analysis performed.

Nuclear knockdown of wildtype TDP43 using shRNAs

Nuclear KD of TDP43 alters the phenotype in differentiated SH-SY5Y cells.
This study has shown that using an overexpression model to cause mislocalization of TDP43 causes a cell phenotype, molecular phenotype and disruptions to miRNA expression. However, the model used has its flaws as it is an overexpression model, therefore the WT TDP43 protein is still present in the nucleus to carry out its role and this does not represent what is observed in the majority of ALS cases, where TDP43 is mainly absent from the nucleus. Therefore, to observe which is more detrimental in vitro, TDP43 mislocalization or absence, a knockdown (KD) of TDP43 was carried out. shRNAs that target the WT TDP43 were designed and cloned into lentiviruses that would target and KD TDP43. Three shRNAs were used, two designed from the coding sequence (CDS 1 and 2) and one from the 3'UTR region of TDP43, a renilla shRNA was used as a control.

The designed TDP43 KD shRNAs were transduced into differentiated SH-SY5Y cells after one week of differentiation, following the same timeline as the mislocalization model. After one week immunostaining and qPCR analysis was performed. Figure 9A shows the average nuclear intensity for TDP43 for each shRNA and B shows the distribution of TDP43 intensities. The data indicates that the CDS 2 shRNA gave a KD of TDP43 protein by around 40% compared to the control. CDS 1 gave a 10% KD and the 3'UTR giving only a 5% KD when each was compared to the control. The distribution of KD was greatest for the 3'UTR, meaning it was the least effective shRNA used for TDP43 KD when compared to the renilla control. The average KD for each CDS shRNA was significant when individually compared to the control by t-test (CDS 1, P=0.0017) (CDS 2, P=0.000021), however the small KD observed for the 3'UTR targeting shRNA was not significant compared to control (P=0.057). The graph in figure 10B showed all differences to be small, but significant ($P \leq 0.0001$), this was likely due to low variance between measurements. As this analysis is looking at protein level, it is unclear if the shRNAs were effective at reducing TDP43. This is as something to be considered is that the conjugated secondary antibody used in immunostaining can bind several times to one primary and

thus give an over exaggerated reading. To confirm TDP43 KD, further qPCR analysis was performed later.

At the same time as staining for TDP43, an antibody for caspase was also used and caspase intensity analysed. The graph in figure 10C shows the average caspase intensity normalised to the renilla control for each of the three shRNAs and the distribution can be viewed in the violin plots in 10D. The shRNA CDS 2 gave an increased caspase reading of 25% compared to control, which was a significant increase (P=0.00029). CDS 1 did not increase significantly compared to the control (9%, NS) and neither did the 3'UTR shRNA (7%, NS). The violin plots showed significant differences for all shRNAs used when each was compared with the control ($P \leq 0.0001$). However, for CDS 2 a higher trend is observed for caspase intensity compared to the control, as opposed to when CDS 1 and the 3'UTR shRNAs were compared to the control, indicating that the larger KD of TDP43 may cause higher levels of apoptosis.

The neuronal network was also analysed as before using TUJ1 as a marker, with the expectation that TDP43 KD would decrease network complexity. The graphs in figures 10E and 10F show that surprisingly for all the shRNAs used there was an increase in neurite outgrowth and branching compared to the renilla control. The data is average outgrowth or number of branches per cell and all data is normalised to the control shown as a line at 1. CDS 1 vs control (Outgrowth P=0.0048, #Branches P=0.00092), CDS 2 vs control (Outgrowth P=0.0065, #Branches P=0.0011) and 3'UTR vs control (Outgrowth P=0.022, #Branches P=0.0022) All showed a significant increase when compared to the control. The 3'UTR shRNA showed less branching and outgrowth and CDS 1 showed the most outgrowth and branching when each was compared to the control. A representative image for network growth (TUJ1) and caspase can be seen in figure 10G for both the renilla control (left) and the CDS 2 shRNA (right). These results did not correlate with TDP43 KD and were unexpected, one explanation may be that the cell line used was a cancer cell line and thus perhaps gave unrealistic results as they are more resilient than primary MNs. The experiment will therefore need to be repeated in MNs.

Figure 10.

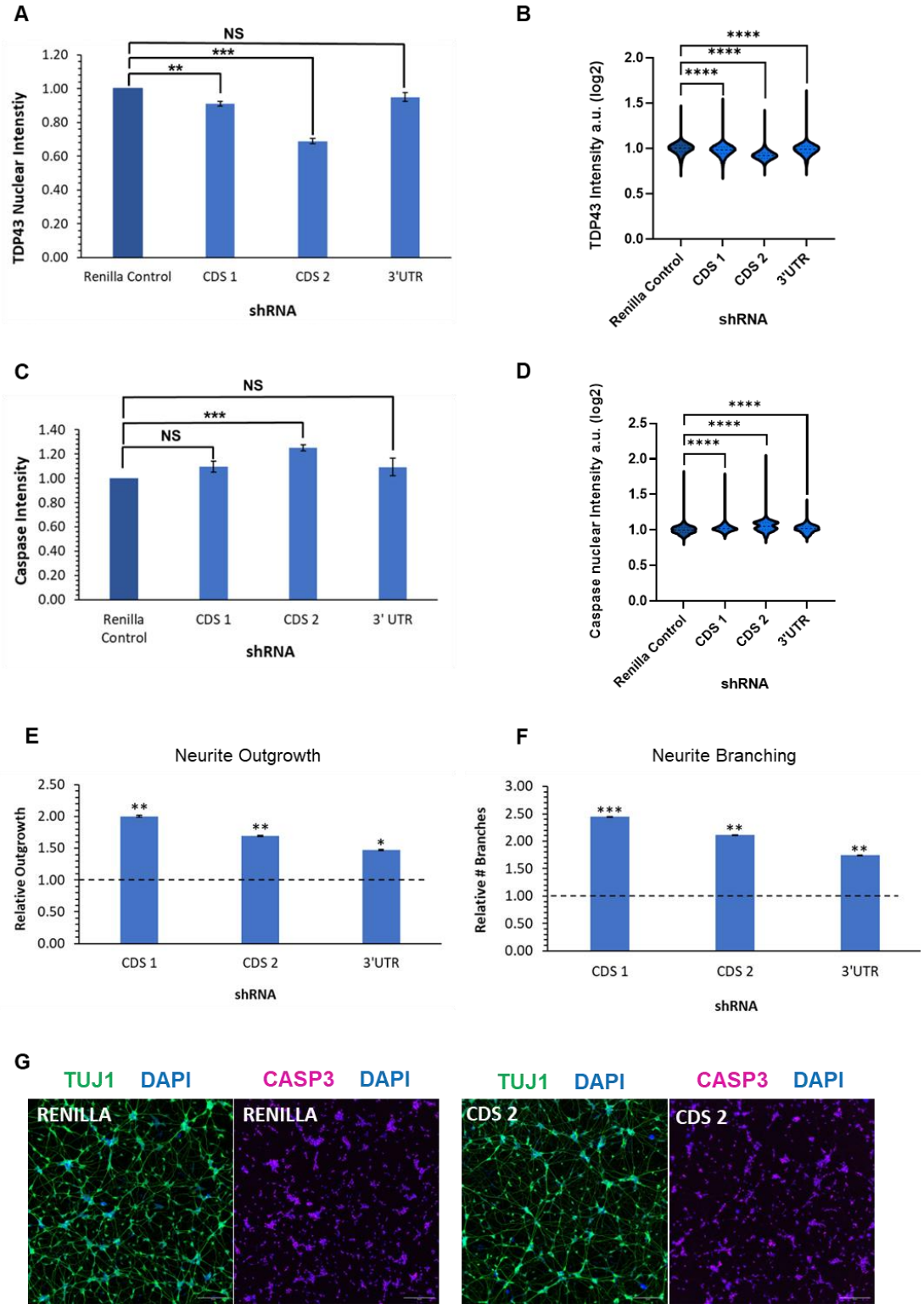
A
NS
***
**
TDP43 Nuclear Intenstiy
1.20
1.00
0.80
0.60
0.40
0.20
0.00
Renilla Control
CDS 1
CDS 2
3'UTR
shRNA
B
****
****
****
TDP43 Intensity a.u. (log2)
2.0
1.5
1.0
0.5
0.0
Renilla Control
CDS 1
CDS 2
3'UTR
shRNA
C
NS
***
NS
Caspase Intensity
1.40
1.20
1.00
0.80
0.60
0.40
0.20
0.00
Renilla Control
CDS 1
CDS 2
3' UTR
shRNA
D
****
****
****
Caspase nuclear Intensity a.u. (log2)
2.5
2.0
1.5
1.0
0.5
0.0
Renilla Control
CDS 1
CDS 2
3'UTR
shRNA
E
Neurite Outgrowth
Relative Outgrowth
2.50
2.00
1.50
1.00
0.50
0.00
**
**
*
CDS 1
CDS 2
3'UTR
shRNA
F
Neurite Branching
Relative # Branches
3.00
2.50
2.00
1.50
1.00
0.50
0.00
***
**
**
CDS 1
CDS 2
3'UTR
shRNA
G
TUJ1
DAPI
CASP3
DAPI
TUJ1
DAPI
CASP3
DAPI
RENILLA
RENILLA
CDS 2
CDS 2

Figure 10. TDP43 knockdown causes a disrupted cell phenotype in differentiated SH-SY5Y cells.

*(A) shRNAs cause knockdown of TDP43 protein in differentiated SH-SY5Y cells. Bar chart shows average TDP43 intensities ± SE normalised to renilla control. T-test analysis was performed to analyse differences between the renilla control and each shRNA, n=3, **P ≤ 0.01, ***P ≤ 0.001, NS = not statistically significant.*

(B) *Violin plot showing the distribution of TDP43 intensities (log2) across all cells for each shRNA. The maximum, minimum and median values shown, and t-test analysis was performed to analyse differences between the control and each shRNA, n=3, ****P ≤ 0.0001.*

(C) *Knockdown of TDP43 in differentiated SH-SY5Y cells causes increased caspase activity. Bar chart shows average caspase intensities ± SE normalised to renilla control. T-test analysis was performed to analyse differences between the control and each shRNA, n=3, ***P ≤ 0.001, NS = not statistically significant.*

(D) *Violin plot showing the distribution of caspase intensities (log2) across all cells for each shRNA. The maximum, minimum and median values shown, and t-test analysis was performed to analyse differences between the control and each shRNA, n=3, ****P ≤ 0.0001.*

*(E+F) Neurite outgrowth and branching analysis following TDP43 KD. Bar charts show average outgrowth and number of branches per cell normalised to renilla control ± SE. Analysis was carried out using TUJ1 marker and PICO analysis software. A t-test was used to analyse differences between the control and each shRNA, n=3, *P ≤ 0.005, **P ≤ 0.01, ***P ≤ 0.001.*

(G) Representative immunofluorescence images following TDP43 KD. Images shown are for renilla control (left) and CDS 2 shRNA (right) using an antibody for TUJ1 (green) and nuclear Hoechst dye (blue). Scale is 106um.

To see if the previous IF results were accurate, qPCR analysis done to look at TDP43 expression. Housekeeping genes for the qPCR were the same as previous and all results have been normalised to the renilla control. Figure 11A shows the relative fold change for the shRNAs and indicates that at a molecular level a higher KD is seen. All shRNAs could significantly KD TDP43 when compared to the control, with the CDS 2 shRNA giving an 80% KD (*P*=3.03E-09). CDS 1 gave a 42% KD vs the control (*P*=5.73429E-09), while the 3'UTR caused a 35% KD when compared to the control (*P*=0.0012). This shows that all the shRNAs can KD TDP43 to some degree when compared individually to the control.

Studies have shown that absence of TDP43 in patients causes certain splicing defects, particularly in the genes STMN2 and UNC13A, that are involved in synapse and microtubule maintenance. Therefore, qPCR analysis was carried out to look at the same genes tested before following the mislocalization model. These were *STMN2*, *STMN2* (TRUNC), *UNC13A,* and *UNC13A* (CE), housekeeping genes were the same as before. Figures 11B-D the gene expression can be observed for the CDS 1, 2 and 3'UTR shRNAs relative to the control. There was a significant decrease in *STMN2* gene expression for the CDS 2 (*P*=4.29E-09) which had an 80% TDP43 KD when compared to the control. While CDS 1 (P=0.035) and the 3'UTR (*P*=0.019) shRNA's showed upregulation, when individually compared to the control, in *STMN2* expression.

The truncated *STMN2* (TRUNC) showed an increase for CDS 1 (3.69, *P*=0.010) and the 3'UTR (3.34, *P*=0.00028). An upregulation was also seen in for the CDS 2 when all were separately compared to the control (26.26, *P*=7.25E-07). *UNC13A* showed a similar trend, with the normal *UNC13A* gene decreasing for CDS 2 (0.88, *P*=0.014). However, it increased slightly for CDS 1 (1.07, *P*=8.62E-06) and the 3'UTR shRNA (1.15, *P*=NS). Finally, the *UNC13A* gene harbouring the CE increased in expression relative to the control for CDS 2 (878.55, *P*=0.00030) correlating with a high TDP43 KD. There was no significant change in *UNC13A* (CE) expression for the CDS 1 and 3'UTR shRNAs (1.11 and 0.63). Perhaps showing that 35-40% level of TDP43 KD (when compared to the control) is not enough to induce a molecular phenotype in these specific genes.

Figure 11.

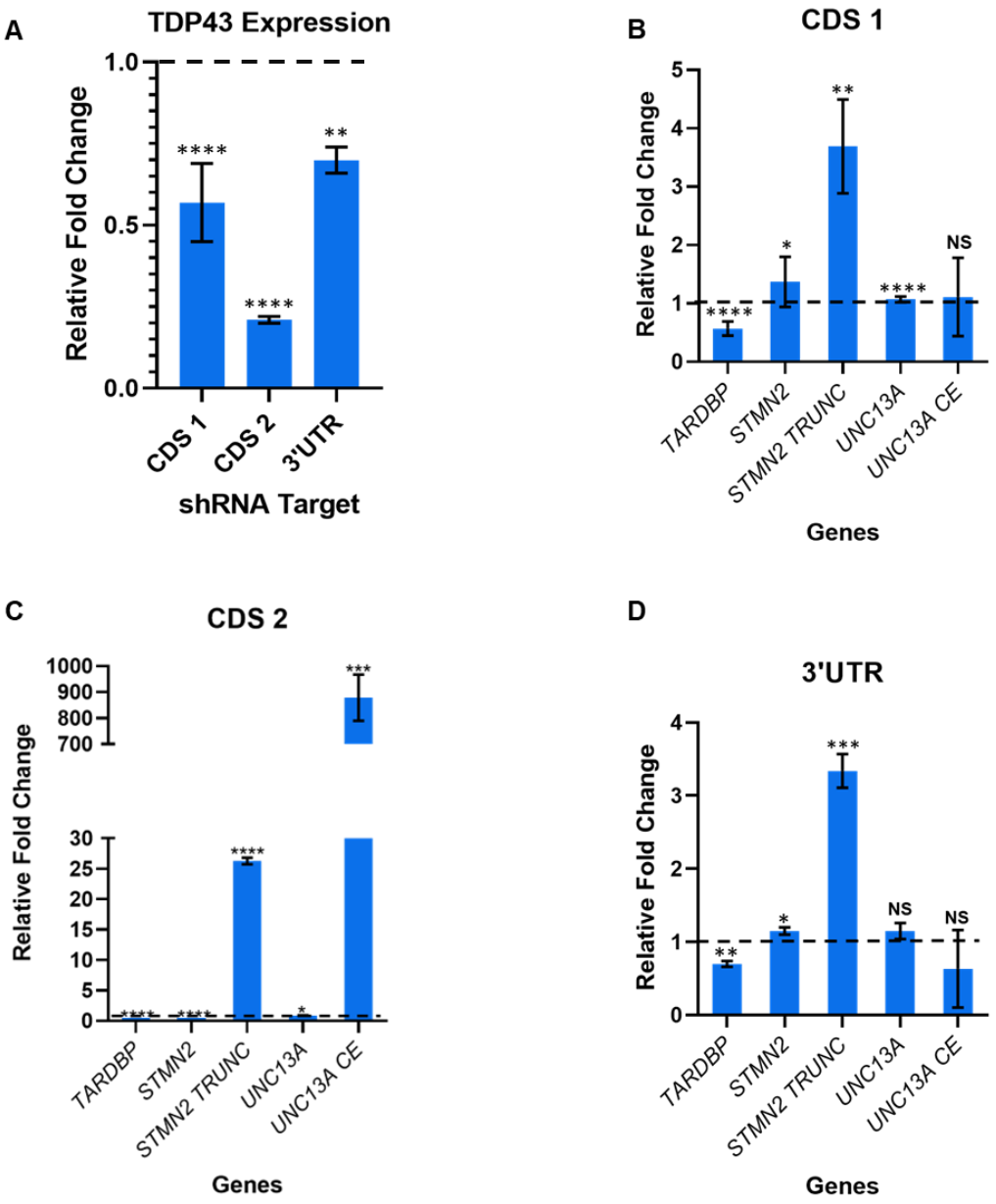
A
TDP43 Expression
Relative Fold Change
1.0
0.5
0.0
****
****
**
CDS 1
CDS 2
3'UTR
shRNA Target
B
CDS 1
Relative Fold Change
5
4
3
2
1
0
****
*
**
****
NS
TARDBP
STMN2
STMN2 TRUNC
UNC13A
UNC13A CE
Genes
C
CDS 2
Relative Fold Change
1000
900
800
700
30
25
20
15
10
5
0
****
****
****
*
***
TARDBP
STMN2
STMN2 TRUNC
UNC13A
UNC13A CE
Genes
D
3'UTR
Relative Fold Change
4
3
2
1
0
**
*
***
NS
NS
TARDBP
STMN2
STMN2 TRUNC
UNC13A
UNC13A CE
Genes

Figure 11. TDP43 knockdown causes a disrupted molecular phenotype in differentiated SH-SY5Y cells.

(A) *qPCR analysis for TDP43 expression individually plotted from graphs B-D. Results presented are relative average fold change ±SE, each shRNA was normalised to renilla control, indicated by the dotted line at 1. A t-test was performed to analyse differences in TDP43 expression, n=3. P-values ≤ 0.05 were considered statistically significant, **P ≤ 0.01, ****P ≤ 0.0001.*

*(B-D) qPCR analysis for genes involved in synapse and microtubule regulation. Results presented are relative average fold change ±SE, each shRNA was normalised to renilla control, indicated by the dotted line at 1. A t-test was performed to analyse differences in gene expression, n=3. P-values ≤ 0.05 were considered statistically significant, *P ≤ 0.05, **P ≤ 0.01, ***P ≤ 0.001, ****P ≤ 0.0001, NS = not statistically significant.*

Nuclear KD of TDP43 alters miRNA profiles in differentiated SH-SY5Y cells. As previously mentioned, miRNAs are known to be altered and dysregulated in several neurodegenerative conditions. The same miRNAs were measured as before following TDP43 mislocalization. The results were different to what was seen with this previous model and can be seen in figure 12 all the shRNAs surprisingly caused increases in miRNA levels compared to the control. The CDS 2 that showed the largest TDP43 KD unexpectedly showed the least disrupted miRNA profiles with the only significant upregulation of over 2-fold being for miR-139 (*P*=2.66E-05). CDS 1 showed significant increases for all the miRNAs tested apart from miR-10a (miR-139: 2.52, *P*=7.23E-05, miR-218: 1.56, *P*=0.00082, miR-9-5p: 1.70, *P*=3.86E-05, miR-342: 1.91, *P*=0.0062) and the 3'UTR caused significant upregulation in all of the miRNAs (miR-139: 2.11, *P*=0.0015, miR-218: 1.98, *P*=0.040, miR-10a: 1.75, *P*=0.044, miR-9-5p: 1.88, *P*=0.022, miR-342: 1.44, *P*=0.0032). This was surprising considering that TDP43 regulates miRNA biogenesis and therefore these findings need to be investigated further to confirm if they are accurate.

Figure 12.

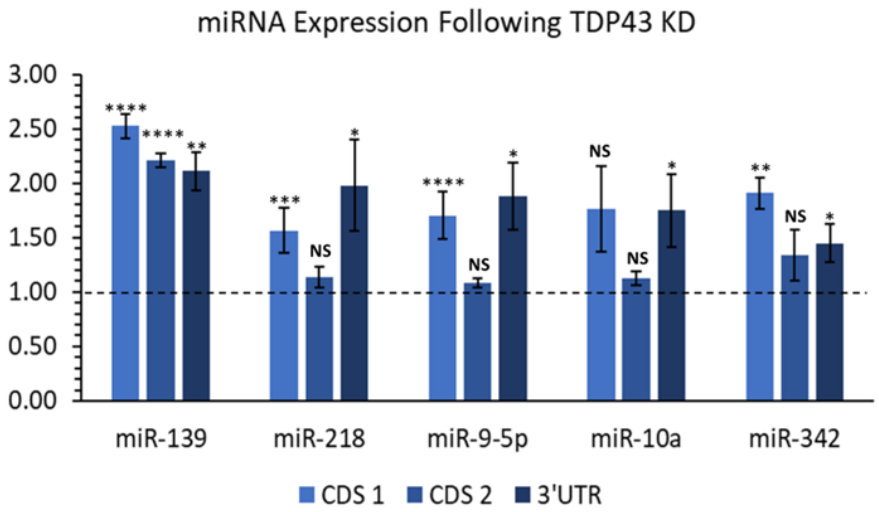

Figure 12. miRNA expression following TDP43 knockdown. *qPCR analysis was performed for several miRNAs following TDP43 KD. Results presented are relative average fold change ±SE, each shRNA was normalised to renilla control, indicated by the dotted line at 1. miRNA expression was normalised to housekeeping genes HPRT1, RNU5 and RNU6. A t-test was performed to analyse differences in miRNA expression, n=3. P-values ≤ 0.05 were considered statistically significant, *P ≤ 0.05, **P ≤ 0.01, ***P ≤ 0.001, ****P ≤ 0.0001, NS = not statistically significant.*

Discussion

Mislocalization of TDP43 causes an altered cell phenotype in SH-SY5Y cells

This study used a model that caused mislocalization of overexpressed TDP43 from the nucleus to the cytoplasm. Models have been developed previously that can cause TDP43 to be mislocalized and many do this by mutating or getting rid of the NLS.(72–75) This study does not alter the NLS, but instead uses a small antibody known as a nanobody, that binds to the eGFP region of overexpressed TDP43-eGFP. The nanobody harbours a strong NES that causes TDP43 mislocalization by overriding the TDP43 NLS. This model successfully mislocalized the overexpressed TDP43 and therefore can be used to investigate what occurs when cytoplasmic TDP43 accumulates. In the mislocalization model, the WT TDP43 is still present in the nucleus and therefore does not depict what is seen in the majority of patients. However, overexpression models are still an effective way of detecting pathways and targets that are affected by a gene or protein of interest.(76)

Neurodegenerative conditions are characterised by an increase in neuron death, eventually leading to disease onset and progression. In ALS for example, it is the degeneration and death of MNs that cause weakening of muscles and paralysis over time as muscle cells can no longer be innervated.(1) The increased cell death is caused by apoptosis, a mechanism of programmed cell death caused by caspase enzymes. Caspases are enzymes that are involved in processes such as proliferation, differentiation, inflammation, but their main role is causing apoptosis.(77) Caspases can be initiators of apoptosis, like caspase-2 or -8 or executioners, for example caspase-3 or -6.(78) Caspase-3 was shown to be increased following TDP43 mislocalization in this study, therefore it is likely that mislocalization of TDP43 is able to trigger the initiation of apoptosis. Increased caspase-3 activity is observed in diseases like ALS and AD.(79,80) This study also shows a link between TDP43 mislocalization and increased caspase-3 activity, thus providing further confirmation that TDP43 cytoplasmic accumulation is likely a key driver of apoptosis in TDP43 proteinopathies.

Diseased neurons also display changes to their morphology compared to healthy neurons, including reduced complexity, shorter axons and less

branching. Following mislocalization of TDP43 using the model described above, the neuronal network was analysed. The data showed a decreasing trend for the number of branches and neurite outgrowth from the control to the mislocalized condition. TDP43 is known to play a role in neuron growth and differentiation, therefore the degeneration observed in diseased neurons may be contributed to by the dysregulation of TDP43 in TDP43 proteinopathies.(81) mislocalization of TDP43 is also known to cause aggregates to form in the cytoplasm, these aggregates have been described to cause defects in neurite growth and differentiation.(82,83) It is unknown if the TDP43-eGFP used in this study was able to form aggregates when mislocalized, but this would explain why neurite branching and outgrowth was decreased. However, future experiments would need to be performed, for example western blot analysis, to confirm if there are any aggregates formed following TDP43 mislocalization.(22) These aggregates are seen in the majority of ALS cases and thus confirmation of aggregate formation would mean the model is representative of the disease even more so.(84)

Investigating miRNA expression and targets following TDP43 dysregulation

Patients with neurodegenerative conditions show dysregulated miRNA profiles and certain miRNAs can even be used as biomarkers.(34,36,85) Differentiated neuroblastoma cells showed altered miRNA expression profiles following TDP43 mislocalization. Several miRNAs were selected based on bioinformatic analysis that looked at dysregulated miRNAs in patients with sporadic ALS. A preliminary qPCR experiment was performed on these miRNAs and those expressed in differentiated SH-SY5Y cells were measured following the use of the nanobody model that can mislocalize TDP43. This study showed all the miRNAs tested were downregulated following TDP43 mislocalization. miR-139, miR-9, miR-10a, miR-29a and miR-342 all gave significantly decreased expression, while miR-218 showed downregulation, but this was not significant. However, an explanation for miR-218s less significant decrease in expression could be due to experiment length as AAVs can take longer to be expressed in post mitotic cells, and in this case, it can take around 7-10 days. Therefore, the result for miR-218 was not ignored, as a downregulation was still observed only a week after transduction, and if left longer this may have become significant.

It is already known that miRNAs are dysregulated in neurodegenerative conditions such as PD, FTD, AD and ALS.(43,50,52,86) miR-10a is enriched in the brain and is decreased in PD models, but when overexpressed it reduces the toxicity in a PD model using SH-SY5Y cells.(52) However, research is lacking looking at this miRNA in the context of other neurodegenerative diseases, like ALS. This study has shown that miR-10a is not only decreased in PD, but may be decreased in other TDP43 proteinopathies, like ALS. miR-9 plays an important regulatory role in dementia and is dysregulated in AD, ALS and other neurodegenerative conditions.(87–90) Its dysregulation across several neurodegenerative conditions may be linked to the TDP43 mislocalization observed across some of these diseases. miR-139 and miR-218 have both been shown to be downregulated in ALS patients, with miR-139 shown to regulate WNT signalling in a recent study.(62,91,92) miR-29a is an important player in AD and can act as a biomarker, but has not been researched in depth relating to other neurodegenerative conditions.(85,89) While miR-342 has been linked to prion diseases, cancer, and fibrosis, while

research is lacking that links miR-342 to neurodegenerative conditions like PD, AD and ALS.(93–95) However, all of these miRNAs are downregulated in differentiated SH-SY5Y cells after TDP43 mislocalization.

TDP43 mislocalization is observed in ALS, dementia, PD and AD and as mentioned above, many miRNAs are dysregulated in these diseases, inclusive of those measured in this study.(12) It could be speculated from this data, that TDP43 being mislocalized to the cytoplasm could be a key factor as to why these miRNAs are shown to be downregulated. Additionally, the downregulation observed is not a full representation of what is seen in patients. The AAVs used in the nanobody model can take up to 10 days to be expressed, therefore this may explain the non-significant result for miR-218. Thus, if the experiment ran longer, it could increase the aberrant miRNA profiles observed. Additionally, the overexpression model used meant the cells still contained WT TDP43. As it is the overexpressed TDP43 that is being mislocalized, the WT would still be in the nuclei. This limitation means that the results seen may be a diluted version of what is seen in vivo, where nuclear TDP43 is depleted. To address this issue, future studies should knock down TDP43 in addition to mislocalization of exogenously expressed TDP43. This will show what is more toxic to cells, high cytoplasmic TDP43, complete knockdown of TDP43, or whether both nuclear knockdown and increase in cytoplasmic TDP43 are required to cause a disease phenotype.

To gain some more insight on the issue raised above, an independent experiment where shRNAs were used to knockdown WT TDP43 was performed. Three shRNAs were transduced into differentiated SH-SY5Y cells following the same timeline used in the mislocalization model. However, instead of overexpression and mislocalization of TDP43, the nuclear WT TDP43 was knocked down. Two of the shRNAs targeted the coding region of TDP43, while one targeted the 3’UTR. The most effective shRNA (CDS 2) knocked TDP43 down by 80%, while the other two knocked it down by 42% (CDS 1) and 30% (3’UTR) respectively. miRNA qPCR analysis was performed following KD using all three shRNAs and the results were surprising. Following KD, miRNA levels all showed to be upregulated, which was unexpected as this is not normally observed as studies have shown KD in certain miRNAs following TDP43 KD.(81,96,97)

Therefore, this study shows that mislocalization is more toxic to miRNA profiles than TDP43 KD. This could be due to the mislocalization perhaps causing aggregation of the protein in the cytoplasm which is seen in patients.(2) It has been shown that TDP43 aggregation can sequester miRNAs, and thus affect gene expression.(98) It is unknown if the model causes aggregate formation, and this could be investigated in future experiments using techniques such as western blotting. The results observed for the miRNA expression after TDP43 KD were unexpected, it could be speculated that TDP43 may regulate some miRNAs in a inhibitory manor and when decreased during KD this causes their upregulation, but this experiment would need to be repeated before such a speculation could be confirmed.

The Wnt and TGF-β/SMAD signalling pathways

After discovery of several miRNAs downregulated following TDP43 mislocalization, a qPCR experiment was run to investigate some of the pathways these miRNAs are involved in to see if these may be altered following miRNA dysregulation. The pathways looked at are known to have involvement of some of the dysregulated miRNAs like miR-10a and miR-29a in the TGF-β/SMAD pathway, and miR-218 and miR-139 in the Wnt signalling pathway and are also involved in neurodegeneration.(61,62,66,67,69,71,99–101) Although no significant results were found due to variability between replicates, there were some obvious trends shown for a number of genes. These included upregulation in the genes *WNT3A, WNT7A, WNT10B* and *ITGA5*, while some downregulation was seen in *WNT4, CCND3, TGF-βI*, *TGF-β1* and *WNT11*. All the other genes that were tested showed no change in expression, therefore those that showed trends in up or downregulation will be discussed in more detail below.

There are 19 Wnt proteins that are involved in the Wnt signalling pathway. These can be canonical, non-canonical or involved in both forms of the Wnt signalling pathway. They are shown to be disrupted in most diseases, inclusive of cancer and neurodegenerative conditions.(60,61,102) It was therefore expected that the Wnt proteins tested would show some dysregulation following TDP43 mislocalization. Though *WNT4* can activate β-catenin, it is also involved in the non-canonical pathway that works independent of β-catenin and has been

shown to promote neuronal differentiation.(103) It was decreased following TDP43 mislocalization, which does not coincide with other studies revealing that β-catenin is increased in neurodegenerative conditions such as ALS.(62) However, *WNT3a* and *WNT10B* appeared to be upregulated, and these are also known to activate β-Catenin signalling.(102) however, interestingly *β-CATENIN* transcript levels did not change following mislocalization and *AXIN2*, which is part of the destruction complex that targets β-Catenin also did not change in expression. Perhaps mislocalization of TDP43 is not enough to alter some of the genes involved in Wnt signalling due to WT TDP43 still being present, and at the same time a TDP43 nuclear KD may provide different gene expression profiles.

Many miRNAs are able to regulate components of the TGF-β/SMAD pathway.(104) However, this pathway can also regulate miRNA biogenesis as the SMAD proteins can bind to the Drosha complex and thus help regulate miRNA production.(105) SMAD signalling is activated during TDP43 mislocalization and it is believed to have a neuroprotective role in preventing TDP43 aggregation.(106) Therefore, if TGF-β/SMAD signalling is altered in neurodegenerative diseases this may be why dysregulated miRNA profiles are seen. Genes tested involved in this pathway showed varied expression. *TGF-β1* and *TGF-βI (TGFBI)* showed no significant change, but a small trend in downregulation was observed. TGF-β1 induces TGF-βI, so the fact they show a similar trend would make sense, but in diseases like ALS and cancer, these are increased to activate pathways and proteins, including SMADs.(65,107,108) as mentioned before, the fact they were unaffected following mislocalization means there must be another or multiple factors that contribute to the variation in *TGF-β* expression seen in neurodegeneration.

Finally, among the genes that did change in expression was a gene known as Integrin Subunit Alpha 5 (*ITGA5*) which was seen to almost triple in expression. This gene codes for the alpha subunit of integrins, which are transmembrane proteins that function as surface adhesion receptors.(109) *ITGA5* is highly expressed in multiple cancers and is involved in promoting metastasis and is upregulated upon TGFβ activation.(110,111) Despite its role in cancer, there is little research that looks at ITGA5, in the field of neurodegeneration. The only gene to show a significant change due to small biological variability was a gene

involved in the cell cycle; *CCND3* (cyclin D3). It was seen to be downregulated following TDP43 mislocalization, which aligns with a study using a model of AD that found *CCND3* to be downregulated and this correlated with neuronal death.(112) However, in other diseases such as cancer, *CCND3* is seen to be increased which causes loss of cell cycle control and further metastasis.(113) *CCND3* is also targeted by several miRNAs, such as miR-194, and these can be used to inhibit and slow cancer progression.(114,115)

These findings highlight the idea that perhaps nuclear KD of TDP43 is required more than or alongside mislocalization to affect gene expression. A qPCR assay could be done using the TDP43 KD samples to see if this is the case. But it is more likely that both mislocalization and KD of TDP43 are required to affect these genes to the same level that occurs in patients. Thus, both methods would need to be combined to achieve this in the future. Regardless, the genes that changed the most, albeit not significantly, were some of the Wnt genes. Two of the miRNAs involved in ALS and Wnt signalling are miR-218 and miR-139, and these were both dysregulated following mislocalization and independent KD of TDP43. Due to already developed techniques by the Bhinge lab, these miRNAs were able to be investigated further to try and uncover potential targets.

miR-218 and DNA methylation

DNA methylation is seen to be increased in neurodegenerative conditions, including ALS.(27,28) The transcript for DNA methylation enzyme DNMT3A was predicted as a direct target of miR-218 by the microRNA target prediction software, Target Scan. SH-SY5Y cells were transfected with two plasmids containing the UTR sequence for *DNMT3A*. One plasmid was the WT containing a miR-218 recognition site, whereas the second contained a mutated version of the recognition site where miR-218 is thought to target (MT). Therefore, in the cells transfected with the MT plasmid, it was expected that miR-218 will be unable to bind and degrade the mRNA for *DNMT3A* and therefore its expression would increase. The data showed increased renilla activity and thus increased *DNMT3A* expression in the MT condition (Figure 8) and therefore it can be speculated that miR-218 targets this gene. However, though the overall trend fit what was expected, there was some biological

variability meaning the result was not significant. Hence, a further experiment was performed to confirm if miR-218 does have a direct effect on the protein levels of *DNMT3A.* However, IF analysis showed no change in DNMT3A protein levels following knockdown and overexpression of miR-218, indicating that miR-218 is not the main miRNA that regulates this transcript.

DNA methylation is a mechanism that can cause gene silencing and is controlled by DNMT enzymes. These enzymes catalyse the transfer of methyl groups to cytosine residues in gene-regulatory regions, such as at promoters and enhancers.(29) It is known that the DNMTs are important in CNS development and neuron differentiation and function.(116) DNMT3A dysregulation has been linked to several disorders, including neuropathic pain, fibrosis, heart failure and several cancers.(117–121) However, its role in neurodegeneration needs to be investigated further, as it has mainly been linked to is ALS. It is shown that the increase in 5-mc caused by hyperactive *DNMT3A* is observed in the blood and spinal cord of ALS patients.(90) It is also described how ALS mice models and cell cultures show MNs increase in apoptosis due to upregulation of *DNMT3A* and *DNMT1* causing increased DNA methylation.(27) Increased DNA methylation is also observed in AD, particularly in late onset AD, with aberrant DNA methylation known to play a role in neurodegeneration.(28,30,31,122,123) Additionally, *DNMT1* mRNA is shown to be increased in PD, but *DNMT3A* levels are unaffected.(124) It is evident that *DNMT3A* has been studied in the context of many diseases, but few studies look at its role in neurodegeneration, inclusive of AD, dementia and ALS. More work needs to be done in this area, as DNA methylation is an important epigenetic mechanism that can alter transcription of all genes, particularly those involved in neurodegenerative conditions.(31)

DNMT3A was of interest in this study due to the fact that its 3’UTR contains two binding regions for miR-218, which is a miRNA known to be decreased in neurodegenerative diseases.(91,92) This study indicates that miR-218 also appears to decrease in expression following TDP43 mislocalization. Consequently, it was speculated that if miR-218 is decreased, then *DNMT3A* expression would be upregulated as miR-218 would no longer target *DNMT3A* mRNA for degradation by RISC. Previous literature supports that this would increase apoptosis in cells, explaining one of the reasons why neurons die in

diseases like ALS.(28) The first experiment performed indicated that miR-218 targets *DNMT3A*, however a further experiment was performed to try and see how perturbation of miR-218 would affect *DNMT3A* in SH-SY5Y neurons. This was to confirm if *DNMT3A* is a main target of miR-218 and how this could play a role in neurodegenerative conditions where miR-218 is dysregulated, like ALS.

miR-218 was independently knocked down and overexpressed in SH-SY5Y cells using two different plasmids along with control plasmids for each condition. Immunostaining was then performed staining for methylation enzyme DNMT3A. Although the luciferase assay indicated that DNMT3A may be a main target of miR-218, the immunostaining showed that this may not be true. As disruption of miR-218 caused no obvious change in DNMT3A intensity and only a small significant difference in DNMT3A signal. The overall distribution indicates that *DNMT3A* is unaffected by miR-218 knockdown or overexpression in-vitro. Target Scan software showed many other miRNAs that may bind *DNMT3A*, and therefore it is likely that one of these regulates the transcript to a higher extent, and thus miR-218 perturbation will not have an important effect on *DNMT3A* expression.

Although *DNMT3A* is apparently not a main target of miR-218, the downregulation of miR-218 still could play a role in MN death. There are many other targets of miR-218. Therefore, these could also be affected by a decrease in miR-218 caused by TDP43 mislocalization. Dysregulation in miR-218 has been linked to multiple cancers, including gastric cancer, which shows that when miR-218 is decreased, it triggers tumour metastasis.(125) A link between miR-218 suppression and increased tumour progression has also been seen in lung cancer.(126) In-vivo studies have shown that miR-218 is involved in developmental pathways, such as the canonical Wnt signalling pathway.(100) This pathway is required in all cells and plays a role in neuronal development.(127) miR-218 has targets within this pathway and therefore if it is not present to regulate them, the Wnt pathway may become dysfunctional leading to impaired neuron development, differentiation and survival. To add, when miR-218 is lost or decreased in cells, it has been shown to cause neuromuscular failure and synaptic dysfunction.(92) These are characteristics of diseases such as ALS and shows that the loss of miR-218 plays a vital role in neurodegeneration. This highlights the importance in understanding TDP43

proteinopathies, as any possible therapeutics that prevent TDP43 mislocalization may be beneficial to several neurodegenerative conditions.

miR-139 and the canonical Wnt signalling pathway

The canonical Wnt signalling pathway is known to be dysregulated in neurodegenerative conditions.(61,128,129) It involves key signalling molecule β-Catenin which is a transcriptional co-activator that helps to control developmental gene expression. In the absence of Wnt, cytoplasmic β-catenin is constantly degraded, but the canonical pathway is activated when a Wnt ligand binds to the receptor, leading to stabilisation of β-Catenin. It can then travel into the nucleus where it helps to co-activate target gene expression.(60) A miRNA that has been found to be decreased in ALS patient spinal cord samples is miR-139 and it is known that Wnt is activated in ALS.(86,128) Recently it has been illustrated that the canonical Wnt signalling pathway may be regulated by miR-139. As when this miRNA is knocked down, it causes upregulation of β-catenin and thus activation of the canonical pathway.(62)

Following overexpression of β-Catenin, activation of apoptosis was investigated by an enzyme called caspase 3 was measured using IF. The results displayed in this study showed an 85% increase in the intensity of this enzyme. Neurodegenerative conditions like ALS are categorised by a large increase in neuronal death. Caspase 3 is one of the caspase enzymes that play a key role in mediating programmed cell death, also known as apoptosis.(78) Caspase 3 is involved in neuronal differentiation and apoptosis, and is seen to be hyperactivated in neurodegenerative conditions like AD.(77–79) Previously the Wnt signalling pathway has been mentioned and its role in neurodegeneration. It is known to be dysregulated in neurodegenerative conditions and in particular has been linked to ALS.(60,61) A recent study has uncovered a finding that links miR-139 to Wnt, specifically the non-canonical Wnt signalling pathway that uses β-Catenin as a key signalling molecule.(62) The study described a feedback mechanism in which miR-139 regulates Wnt signalling, and when depleted it causes hyperactivation of Wnt and an increase in β-Catenin.(62)

β-Catenin is involved in regulating many pathways and in neurons is involved in cell survival and proliferation.(60) Studies have shown that increased activity of β-Catenin can cause an increase in apoptosis and tumour growth in diseases

such as cancer.(130,131) This study has shown that this increase of apoptosis due to increased β-Catenin may also be applicable to neurodegeneration. Targeting Wnt signalling as a therapeutic strategy in disease has been spoken about widely in research. However, this pathway is extremely important in regulating many cell functions and any drugs that target parts of this pathway may cause off-target side effects.(132) This study provides more evidence as to why targeting miRNAs may be a safer and still beneficial therapeutic approach. However, there will still be hurdles to overcome, for example some miRNAs can have many targets, therefore more research needs to be conducted before considering this approach

Gene regulation and splicing defects following TDP43 dysregulation

Depletion of RNA binding protein TDP43 is a hallmark of many neurodegenerative conditions, particularly in dementia and ALS. The loss of this protein has been shown to cause splicing defects within cells as mentioned earlier.(13,23) Two proteins affected by loss of TDP43 are the UNC13A protein and stathmin-2 protein. The UNC13 protein is involved in vesicle priming and neurotransmitter release and is therefore critical for signalling at the NMJ, while stathmin-2 is involved in microtubule regulation and thus neuronal growth.(21,23) TDP43 plays a role in suppressing cryptic exons, these are exons that are usually excluded from mature mRNA, and when TDP43 is depleted they are included.(23,133,134) The inclusion of a cryptic exon in the *UNC13A* gene means the UNC13A protein is not produced which can be detrimental for synaptic functioning.(23) The inclusion of a cryptic exon in the *STMN2* gene introduces a premature stop codon and therefore leads to a truncated version of the STMN2 protein, which disturbs normal neuron growth and contributes to neurodegeneration.(21,22,24) Thus the loss of TDP43 can cause both of these mutated genes to occur and may be detrimental to neuronal functioning and growth.

During this study a model was used that overexpressed and mislocalized TDP43 and in a later independent experiment TDP43 was also knocked down. Following both methods of TDP43 perturbation qPCR was performed to measure the *UNC13A* and *STMN2* genes, as well as their mutated counterparts that are caused by the inclusion of said cryptic exons. The data obtained demonstrates that these genes are unaffected by the mislocalization of TDP43, and this was likely due to the continued presence of WT TDP43 in the nucleus. However, it also shows that the cytoplasmic increase of TDP43 does not have an effect on these splicing events and the expression of these genes, like it seems to have on miRNA expression. As expected however, the KD of WT TDP43 has an impact on these genes and this coincides with what is observed in current literature.(23,24) The majority of ALS patients experience TDP43 pathology (around 97%) with the severity ranging across patients and is said to correlate with the stages of disease progression.(135,136)

In this study shRNAs were used to KD TDP43 and following qPCR analysis the genes *STMN2* and *UNC13A* were seen to be decreased. As STMN2 protein is involved in neuron growth and repair, it would be expected that neurite growth and branching would decrease following TDP43 KD and STMN2 dysregulation, but analysis surprisingly showed increased neurite branching and outgrowth. This did not fit with previous work on primary neurons that reported the opposite following altered *STMN2* expression.(21,137) This result was also different to what was observed following the mislocalization model where neurite growth and branching showed a decreased trend after mislocalization. Both KD and mislocalization of TDP43 have been shown to cause reduced neuron growth and complexity.(138) It is therefore unclear as to why an increase was observed following KD, but in future studies a more appropriate post mitotic cell type could be used to represent disease better, for example primary MNs. Yet, in this study, TDP43 overexpression and mislocalization seems to be more detrimental to neurite growth and branching than KD.

Interestingly the three shRNAs that were utilised in this study to KD TDP43 all cause different amounts of KD, one being 80%, another 42% and the one only causing a 35% decrease in TDP43 expression. The degree of KD correlates with caspase activity and gene expression which can clearly be seen for the cryptic exon versions of *STMN2* and *UNC13A*. When TDP43 KD increased so did the expression of truncated *STMN2* and *UNC13A CE.* Importantly, this study shows that nuclear loss is essential for these gene deficits to occur, as mislocalization alone showed no alteration in the expression of these genes, where WT TDP43 was still present in the nucleus. Therefore, splicing defects increase due to loss of nuclear TDP43, and this study may also show that a loss of around 40% TDP43 is when these defects start to become apparent. Supporting the idea that TDP43 pathology correlates with stages of disease progression.(136)

Conclusions, Limitations and Future Direction

In conclusion, TDP43 dysregulation plays a key role in neurodegenerative conditions, particularly ALS. Mislocalization of overexpressed TDP43 causes downregulation of miRNAs and thus dysregulation in miRNA processing as well as in neuronal growth processes. miRNAs such as miR-218 and miR-139 play clear roles in neurodegeneration, although the exact role of miR-218 needs to be investigated further, especially as it is the most down regulated miRNA in ALS. Other miRNAs that were also seen to be dysregulated could also be potential therapeutic targets for neurodegenerative conditions, but until their roles are studied at a deeper level this will remain unknown. miR-9, miR-10a and miR-342 are promising targets as all are highly dysregulated due to TDP43 mislocalization and KD and are involved in several degenerative conditions. Therefore, therapies targeting miRNAs could be a promising option as it would benefit all TDP43 proteinopathies.

One limitation in this project was time. A key thing that needs to be considered for future work is transcriptome and miRNAome analysis. Following use of this model these could be carried out to identify all genes and miRNAs that may be affected following TDP-43 mislocalization. This would be a big step in identifying any new genes or miRNAs that have not yet been linked to neurodegenerative conditions such as ALS. qPCR was used as the main approach to look at gene expression, however it may not have been optimal, as although it is assumed that HK genes remain constant between groups, it is not guaranteed. Transcriptomics would have been more reliable and a higher standard approach, however due to time restraints qPCR was performed and 3-5 HK genes used to try and mitigate any changes in HK expression.

TDP43 KD also causes miRNA dysregulation, but more so affects splicing of genes because of TDP43 nuclear loss. This nuclear depletion is essential to cause splicing defects, and this study indicates there may be a threshold of at least 40% loss of *TARDBP* expression required to cause cryptic exon inclusion in genes. Indicating that neurodegeneration increases alongside TDP43 pathology progression. Both nuclear loss and cytoplasmic gain of the protein are therefore toxic as they cause disruptions in different processes. Hence, different therapies may be required either targeting the nuclear loss or

cytoplasmic gain as individual pathways are affected by each. Patients show a varying range of TDP43 mislocalization, likely based on disease progression, thus indicating a challenge of timing when giving any new therapies. This will be important depending on which pathways you want to target based on severity of TDP43 pathology. miRNAs seem to be a promising new approach as they are implicated in several conditions, can easily be perturbed and could even be used as a therapy themself. However, there is also the possibility of off-target effects as what was observed in this study for miR-218, miRNAs can target several genes and their perturbation can affect some but not others and therefore this still needs to be investigated.

As mentioned previously TDP43 is seen to be both downregulated and mislocalized in patients and therefore, future experiments need to be conducted to create a more accurate disease model. A shared limitation in these models was the low efficiency of TDP43 knockdown and mislocalization. This could be improved by using genome editing, and cell sorting by either GFP positive cells or by using a selective marker. This would create a cell line that efficiently displayed TDP-43 knockdown or/and mislocalization that could be used to future experiments. Such a cell line would be best made using iPSC-derived MNs. This project used SH-SY5Y cells, which are a cancer cell line and therefore will not behave the same as patient neurons, although they can be used for proof of concept work, any future work should focus on iPSC-derived MNs. This is because conditions like ALS affect a specific cell type, MNs, and these cells may have different regulatory networks or genes expressed that are not present in SH-SY5Y cells, yet contribute to disease pathology.(139) The next step would be to combine the methods in this study to KD and cause mislocalization of TDP43 in iPSC-derived MNs. This would create an accurate in-vitro model of TDP43 dysregulation and would enable investigation of any further miRNAs, splicing defects and linked pathways involved in these debilitating neurodegenerative TDP43 proteinopathies.

Appendices

Gene Target	Sequence	Forward	Reverse
TARDBP CDS 1 (Exon 6)	GCTCTAA TTCTGGT GCAGCAA	5'-GATCCGCTCTAATTCTG GTGCAGCAACTCGAGTT GCTGCACCAGAATTAGA GCTTTTTG-3'	5'-AATTCAAAAAGCTCTA ATTCTGGTGCAGCAA CTCGAGTTGCTGCAC CAGAATTAGAGCG-3'
TARDBP CDS 2 (Exon 6)	GCAATAG ACAGTTA GAAAGAA	5'-GATCCGCAATAGACAGT TAGAAAGAACTCGAGTT CTTTCTAACTGTCTATTG CTTTTTG-3'	5'-AATTCAAAAAGCAATA GACAGTTAGAAAGAA CTCGAGTTCTTTCTAA CTGTCTATTGCG-3'
TARDBP 3' UTR	TCTAAAC TCATGGT AAGTATA	5'-GATCCTCTAAACTCATG GTAAGTATACTCGAGTA TACTTACCATGAGTTTAG ATTTTTG-3'	5'-AATTCAAAAATCTAAA CTCATGGTAAGTATA CTCGAGTATACTTAC CATGAGTTTAGAG-3'

Table 1. Primer sequences for knockdown shRNAs.

Antibody	*Species*	*Dilution*	*Company (Catalogue #)*
Primary:			
TDP43	*Rabbit*	*1:800*	*ProteinTech (10782-2-AP)*
Caspase 3	*Rabbit*	*1:400*	*Cell Signalling Technologies (9664L)*
GFP	*Goat*	*1:800*	*Santa Cruz Biotech (sc-5385)*
MAP2	*Chicken*	*1:16000*	*GeneTex (GTX82661)*
TUJ1	*Mouse*	*1:1000*	*BioLegend (MMS-435P-100)*
DNMT3A	*Rabbit*	*1:1000*	*GeneTex (GTX129125)*
Secondary:			
Anti-Rb	*Goat*	*1:2000*	*Abcam, UK (ab150083)*
Anti-Ms	*Donkey*	*1:2000*	*Abcam, UK (ab150105)*
Anti-Ck	*Goat*	*1:2000*	*Abcam, UK (ab150176)*
Anti-Go	*Donkey*	*1:2000*	*Abcam, UK (ab150129)*

Table 2. Antibodies used for immunostaining.

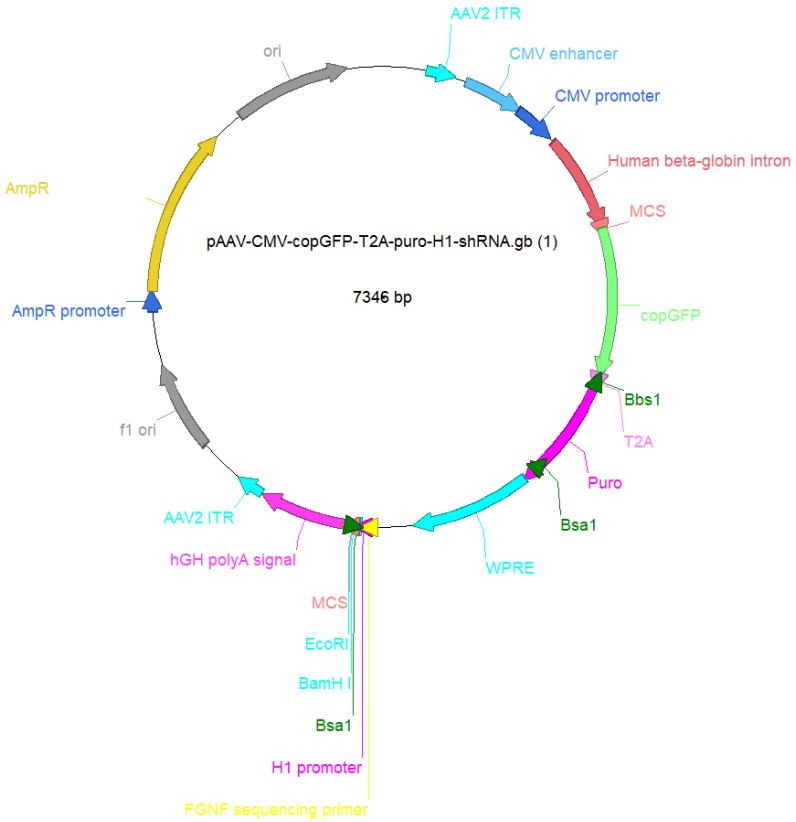

Figure 1. pAAV-cmv-gfp-h1-mir218 plasmid map. *Backbone plasmid used to clone the miR-218 overexpression shRNA, visual created on ApE. Digested with enzymes ECOR1 and BAMH1 and cloned using T4 ligation by Dr Sophie Hawkins prior to use on this project. Oligonucleotides sequences for hsa-miR-218-5p were Forward: 5'-GATCCACATGGTTAGATCAAGCACAATTCAAGAGATTGTGCTTGATCTAACCATGTTTTTTG-3', Reverse: 5'-AATTCAAAAAACATGGTTAGATCAAGCACAATCTCTTGAATTGTGCTTGATCTAACCATGTG-3'.*

References

1. Brown RH, Al-Chalabi A. Amyotrophic Lateral Sclerosis. N Engl J Med. 2017 Jul 13;377(2):162–72.

2. Suk TR, Rousseaux MWC. The role of TDP-43 mislocalization in amyotrophic lateral sclerosis. Mol Neurodegener. 2020 Aug 15;15(1):45.

3. Andrews JA, Jackson CE, Heiman-Patterson TD, Bettica P, Brooks BR, Pioro EP. Real-world evidence of riluzole effectiveness in treating amyotrophic lateral sclerosis. Amyotroph Lateral Scler Frontotemporal Degener. 2020 Nov;21(7-8):509–18.

4. Bucchia M, Ramirez A, Parente V, Simone C, Nizzardo M, Magri F, et al. Therapeutic development in amyotrophic lateral sclerosis. Clin Ther. 2015 Mar 1;37(3):668–80.

5. Butti Z, Patten SA. RNA Dysregulation in Amyotrophic Lateral Sclerosis [Internet]. Vol. 9, Frontiers in Genetics. 2019. Available from: http://dx.doi.org/10.3389/fgene.2018.00712

6. Kaur SJ, McKeown SR, Rashid S. Mutant SOD1 mediated pathogenesis of Amyotrophic Lateral Sclerosis. Gene. 2016 Feb 15;577(2):109–18.

7. Blair IP, Williams KL, Warraich ST, Durnall JC, Thoeng AD, Manavis J, et al. FUS mutations in amyotrophic lateral sclerosis: clinical, pathological, neurophysiological and genetic analysis. J Neurol Neurosurg Psychiatry. 2010 Jun;81(6):639–45.

8. Prasad A, Bharathi V, Sivalingam V, Girdhar A, Patel BK. Molecular Mechanisms of TDP-43 Misfolding and Pathology in Amyotrophic Lateral Sclerosis. Front Mol Neurosci. 2019 Feb 14;12:25.

9. Tziortzouda P, Van Den Bosch L, Hirth F. Triad of TDP43 control in neurodegeneration: autoregulation, localization and aggregation. Nat Rev Neurosci. 2021 Apr;22(4):197–208.

10. François-Moutal L, Perez-Miller S, Scott DD, Miranda VG, Mollasalehi N, Khanna M. Structural Insights Into TDP-43 and Effects of Post-translational Modifications. Front Mol Neurosci. 2019 Dec 17;12:301.

11. Lagier-Tourenne C, Cleveland DW. Rethinking ALS: the FUS about TDP-43. Cell. 2009 Mar 20;136(6):1001–4.

12. Gao J, Wang L, Yan T, Perry G, Wang X. TDP-43 proteinopathy and mitochondrial abnormalities in neurodegeneration. Mol Cell Neurosci. 2019 Oct;100:103396.

13. Buratti E, Baralle FE. Multiple roles of TDP-43 in gene expression, splicing regulation, and human disease. Front Biosci. 2008 Jan 1;13:867–78.

14. Hergesheimer RC, Chami AA, de Assis DR, Vourc'h P, Andres CR, Corcia P, et al. The debated toxic role of aggregated TDP-43 in amyotrophic lateral sclerosis: a resolution in sight? Brain. 2019 May 1;142(5):1176–94.

15. Duan W, Li X, Shi J, Guo Y, Li Z, Li C. Mutant TAR DNA-binding protein-43 induces oxidative injury in motor neuron-like cell. Neuroscience. 2010 Sep 15;169(4):1621–9.

16. Barmada SJ, Skibinski G, Korb E, Rao EJ, Wu JY, Finkbeiner S. Cytoplasmic mislocalization of TDP-43 is toxic to neurons and enhanced by a mutation associated with familial amyotrophic lateral sclerosis. J Neurosci. 2010 Jan 13;30(2):639–49.

17. Sasaguri H, Chew J, Xu YF, Gendron TF, Garrett A, Lee CW, et al. The extreme N-terminus of TDP-43 mediates the cytoplasmic aggregation of TDP-43 and associated toxicity in vivo. Brain Res. 2016 Sep 15;1647:57–64.

18. Montalbano M, McAllen S, Cascio FL, Sengupta U, Garcia S, Bhatt N, et al. TDP-43 and Tau Oligomers in Alzheimer's Disease, Amyotrophic Lateral Sclerosis, and Frontotemporal Dementia. Neurobiol Dis. 2020 Dec;146:105130.

19. Gu J, Chen F, Iqbal K, Gong CX, Wang X, Liu F. Transactive response DNA-binding protein 43 (TDP-43) regulates alternative splicing of tau exon 10: Implications for the pathogenesis of tauopathies. J Biol Chem. 2017 Jun 23;292(25):10600–12.

20. Halim D, Gao FB. RNA targets of TDP-43: Which one is more important in neurodegeneration? Transl Neurodegener. 2022 Feb 25;11(1):12.

21. Klim JR, Williams LA, Limone F, Guerra San Juan I, Davis-Dusenbery BN, Mordes DA, et al. ALS-implicated protein TDP-43 sustains levels of STMN2, a mediator of motor neuron growth and repair. Nat Neurosci. 2019 Feb;22(2):167–79.

22. Guerra San Juan I, Nash LA, Smith KS, Leyton-Jaimes MF, Qian M, Klim JR, et al. Loss of mouse Stmn2 function causes motor neuropathy. Neuron. 2022 May 18;110(10):1671–88.e6.

23. Ma XR, Prudencio M, Koike Y, Vatsavayai SC, Kim G, Harbinski F, et al. TDP-43 represses cryptic exon inclusion in the FTD-ALS gene UNC13A. Nature. 2022 Mar;603(7899):124–30.

24. Prudencio M, Humphrey J, Pickles S, Brown AL, Hill SE, Kachergus JM, et al. Truncated stathmin-2 is a marker of TDP-43 pathology in frontotemporal dementia. J Clin Invest. 2020 Nov 2;130(11):6080–92.

25. Appleby-Mallinder C, Schaber E, Kirby J, Shaw PJ, Cooper-Knock J, Heath PR, et al. TDP43 proteinopathy is associated with aberrant DNA methylation in human amyotrophic lateral sclerosis. Neuropathol Appl Neurobiol. 2021 Feb;47(1):61–72.

26. Štalekar M, Yin X, Rebolj K, Darovic S, Troakes C, Mayr M, et al. Proteomic analyses reveal that loss of TDP-43 affects RNA processing and intracellular transport. Neuroscience. 2015 May 7;293:157–70.

27. Chestnut BA, Chang Q, Price A, Lesuisse C, Wong M, Martin LJ. Epigenetic regulation of motor neuron cell death through DNA methylation. J Neurosci. 2011 Nov 16;31(46):16619–36.

28. Martin LJ, Wong M. Aberrant regulation of DNA methylation in amyotrophic lateral sclerosis: a new target of disease mechanisms. Neurotherapeutics. 2013 Oct;10(4):722–33.

29. Moore LD, Le T, Fan G. DNA methylation and its basic function. Neuropsychopharmacology. 2013 Jan;38(1):23–38.

30. Chouliaras L, Kenis G, Visser PJ, Scheltens P, Tsolaki M, Jones RW, et al. DNMT3A moderates cognitive decline in subjects with mild cognitive impairment: replicated evidence from two mild cognitive impairment cohorts. Epigenomics. 2015;7(4):533–7.

31. Martínez-Iglesias O, Carrera I, Carril JC, Fernández-Novoa L, Cacabelos N, Cacabelos R. DNA Methylation in Neurodegenerative and Cerebrovascular Disorders. Int J Mol Sci [Internet]. 2020 Mar 23;21(6). Available from: http://dx.doi.org/10.3390/ijms21062220

32. Quinlan S, Kenny A, Medina M, Engel T, Jimenez-Mateos EM. MicroRNAs in Neurodegenerative Diseases. Int Rev Cell Mol Biol. 2017 Jun 16;334:309–43.

33. Campos-Melo D, Droppelmann CA, He Z, Volkening K, Strong MJ. Altered microRNA expression profile in Amyotrophic Lateral Sclerosis: a role in the regulation of NFL mRNA levels. Mol Brain. 2013 May 24;6:26.

34. Dardiotis E, Aloizou AM, Siokas V, Patrinos GP, Deretzi G, Mitsias P, et al. The Role of MicroRNAs in Patients with Amyotrophic Lateral Sclerosis. J Mol Neurosci. 2018 Dec;66(4):617–28.

35. Kawahara Y, Mieda-Sato A. TDP-43 promotes microRNA biogenesis as a component of the Drosha and Dicer complexes. Proc Natl Acad Sci U S A. 2012 Feb 28;109(9):3347–52.

36. Paez-Colasante X, Figueroa-Romero C, Rumora AE, Hur J, Mendelson FE, Hayes JM, et al. Cytoplasmic TDP43 Binds microRNAs: New Disease Targets in Amyotrophic Lateral Sclerosis. Front Cell Neurosci. 2020 May 12;14:117.

37. Lagos-Quintana M, Rauhut R, Lendeckel W, Tuschl T. Identification of novel genes coding for small expressed RNAs. Science. 2001 Oct 26;294(5543):853–8.

38. Soliman AM, Das S, Abd Ghafar N, Teoh SL. Role of MicroRNA in Proliferation Phase of Wound Healing. Front Genet. 2018 Feb 14;9:38.

39. Kehl T, Backes C, Kern F, Fehlmann T, Ludwig N, Meese E, et al. About miRNAs, miRNA seeds, target genes and target pathways. Oncotarget. 2017 Dec 5;8(63):107167–75.

40. Bartel DP. MicroRNAs: target recognition and regulatory functions. Cell. 2009 Jan 23;136(2):215–33.

41. Bartel DP. MicroRNAs: genomics, biogenesis, mechanism, and function. Cell. 2004 Jan 23;116(2):281–97.

42. O'Brien J, Hayder H, Zayed Y, Peng C. Overview of MicroRNA Biogenesis, Mechanisms of Actions, and Circulation. Front Endocrinol . 2018 Aug 3;9:402.

43. Emde A, Eitan C, Liou LL, Libby RT, Rivkin N, Magen I, et al. Dysregulated miRNA biogenesis downstream of cellular stress and ALS-causing mutations: a new mechanism for ALS. EMBO J. 2015 Nov 3;34(21):2633–51.

44. Winter J, Jung S, Keller S, Gregory RI, Diederichs S. Many roads to maturity: microRNA biogenesis pathways and their regulation. Nat Cell Biol. 2009 Mar;11(3):228–34.

45. Yoshino H, Yonemori M, Miyamoto K, Tatarano S, Kofuji S, Nohata N, et al. microRNA-210-3p depletion by CRISPR/Cas9 promoted tumorigenesis through revival of TWIST1 in renal cell carcinoma. Oncotarget. 2017 Mar 28;8(13):20881–94.

46. Ho TT, Zhou N, Huang J, Koirala P, Xu M, Fung R, et al. Targeting non-coding RNAs with the CRISPR/Cas9 system in human cell lines. Nucleic Acids Res. 2015 Feb 18;43(3):e17.

47. Stenvang J, Petri A, Lindow M, Obad S, Kauppinen S. Inhibition of microRNA function by antimiR oligonucleotides. Silence. 2012 Jan 9;3(1):1.

48. Ebert MS, Sharp PA. MicroRNA sponges: progress and possibilities. RNA. 2010 Nov;16(11):2043–50.

49. Liu J, Zhou F, Guan Y, Meng F, Zhao Z, Su Q, et al. The Biogenesis of miRNAs and Their Role in the Development of Amyotrophic Lateral Sclerosis. Cells [Internet]. 2022 Feb 7;11(3). Available from: http://dx.doi.org/10.3390/cells11030572

50. Rizzuti M, Filosa G, Melzi V, Calandriello L, Dioni L, Bollati V, et al. MicroRNA expression analysis identifies a subset of downregulated miRNAs in ALS motor neuron progenitors. Sci Rep. 2018 Jul 4;8(1):10105.

51. Hoye ML, Koval ED, Wegener AJ, Hyman TS, Yang C, O'Brien DR, et al. MicroRNA Profiling Reveals Marker of Motor Neuron Disease in ALS Models. J Neurosci. 2017 May 31;37(22):5574–86.

52. Liang H, Ding B, Liang J, Shi X, Jiang X, Gao Y. MicroRNA-10a inhibits A30P α-synuclein aggregation and toxicity by targeting proapoptotic protein BCL2L11. Int J Clin Exp Pathol. 2018 Feb 1;11(2):624–33.

53. Liu Y, Zhang Y, Wu H, Li Y, Zhang Y, Liu M, et al. miR-10a suppresses colorectal cancer metastasis by modulating the epithelial-to-mesenchymal transition and anoikis. Cell Death Dis. 2017 Apr 6;8(4):e2739.

54. Setijono SR, Park M, Kim G, Kim Y, Cho KW, Song SJ. miR-218 and miR-129 regulate breast cancer progression by targeting Lamins. Biochem Biophys Res Commun. 2018 Feb 12;496(3):826–33.

55. Zhang H da, Jiang LH, Sun DW, Li J, Tang JH. MiR-139-5p: promising biomarker for cancer. Tumour Biol. 2015 Mar;36(3):1355–65.

56. Liu B, Tian Y, Li F, Zhao Z, Jiang X, Zhai C, et al. Tumor-suppressing roles of miR-214 and miR-218 in breast cancer. Oncol Rep. 2016 Jun;35(6):3178–84.

57. Wang S, Wu W, Claret FX. Mutual regulation of microRNAs and DNA methylation in human cancers. Epigenetics. 2017 Mar 4;12(3):187–97.

58. Liu Y, Huang T, Zhao X, Cheng L. MicroRNAs modulate the Wnt signaling pathway through targeting its inhibitors. Biochem Biophys Res Commun. 2011 May 6;408(2):259–64.

59. Redshaw N, Camps C, Sharma V, Motallebipour M, Guzman-Ayala M, Oikonomopoulos S, et al. TGF-β/Smad2/3 signaling directly regulates several miRNAs in mouse ES cells and early embryos. PLoS One. 2013 Jan 30;8(1):e55186.

60. MacDonald BT, Tamai K, He X. Wnt/beta-catenin signaling: components, mechanisms, and diseases. Dev Cell. 2009 Jul;17(1):9–26.

61. Clevers H, Nusse R. Wnt/β-catenin signaling and disease. Cell. 2012 Jun 8;149(6):1192–205.

62. Hawkins S, Namboori SC, Tariq A, Blaker C, Flaxman C, Dey NS, et al. Upregulation of β-catenin due to loss of miR-139 contributes to motor neuron death in amyotrophic lateral sclerosis. Stem Cell Reports [Internet]. 2022 Jun 9; Available from: http://dx.doi.org/10.1016/j.stemcr.2022.05.019

63. Akhurst RJ, Hata A. Targeting the TGFβ signalling pathway in disease. Nat Rev Drug Discov. 2012 Oct;11(10):790–811.

64. Burks TN, Cohn RD. Role of TGF-β signaling in inherited and acquired myopathies. Skelet Muscle. 2011 May 4;1(1):19.

65. von Bernhardi R, Cornejo F, Parada GE, Eugenín J. Role of TGFβ signaling in the pathogenesis of Alzheimer's disease. Front Cell Neurosci. 2015 Oct 28;9:426.

66. Muñoz MD, de la Fuente N, Sánchez-Capelo A. TGF-β/Smad3 Signalling Modulates GABA Neurotransmission: Implications in Parkinson's Disease. Int J Mol Sci [Internet]. 2020 Jan 16;21(2). Available from: http://dx.doi.org/10.3390/ijms21020590

67. Katsuno M, Adachi H, Banno H, Suzuki K, Tanaka F, Sobue G. Transforming growth factor-β signaling in motor neuron diseases. Curr Mol Med. 2011 Feb;11(1):48–56.

68. Xu F, Liu C, Zhou D, Zhang L. TGF-β/SMAD Pathway and Its Regulation in Hepatic Fibrosis. J Histochem Cytochem. 2016 Mar;64(3):157–67.

69. Tang PMK, Lan HY. MicroRNAs in TGF-β/Smad-mediated Tissue Fibrosis. Curr Pathobiol Rep. 2014 Dec 1;2(4):235–43.

70. Zhou G, Lin W, Fang P, Lin X, Zhuge L, Hu Z, et al. MiR-10a improves hepatic fibrosis by regulating the TGFβl/Smads signal transduction pathway. Exp Ther Med. 2016 Sep;12(3):1719–22.

71. Li PF, He RH, Shi SB, Li R, Wang QT, Rao GT, et al. Modulation of miR-10a-mediated TGF-β1/Smads signaling affects atrial fibrillation-induced cardiac fibrosis and cardiac fibroblast proliferation. Biosci Rep [Internet]. 2019 Feb 28;39(2). Available from: http://dx.doi.org/10.1042/BSR20181931

72. Jo M, Lee S, Jeon YM, Kim S, Kwon Y, Kim HJ. The role of TDP-43 propagation in neurodegenerative diseases: integrating insights from clinical and experimental studies. Exp Mol Med. 2020 Oct;52(10):1652–62.

73. Atkinson R, Leung J, Bender J, Kirkcaldie M, Vickers J, King A. TDP-43 mislocalization drives neurofilament changes in a novel model of TDP-43 proteinopathy. Dis Model Mech [Internet]. 2021 Jan 6; Available from: http://dx.doi.org/10.1242/dmm.047548

74. Dyer MS, Reale LA, Lewis KE, Walker AK, Dickson TC, Woodhouse A, et al. Mislocalisation of TDP-43 to the cytoplasm causes cortical hyperexcitability and reduced excitatory neurotransmission in the motor cortex. J Neurochem. 2021 May;157(4):1300–15.

75. Dyer MS, Woodhouse A, Blizzard CA. Cytoplasmic Human TDP-43 Mislocalization Induces Widespread Dendritic Spine Loss in Mouse Upper Motor Neurons. Brain Sci [Internet]. 2021 Jun 30;11(7). Available from: http://dx.doi.org/10.3390/brainsci11070883

76. Prelich G. Gene overexpression: uses, mechanisms, and interpretation. Genetics. 2012 Mar;190(3):841–54.

77. D'Amelio M, Cavallucci V, Cecconi F. Neuronal caspase-3 signaling: not only cell death. Cell Death Differ. 2010 Jul;17(7):1104–14.

78. Asadi M, Taghizadeh S, Kaviani E, Vakili O, Taheri-Anganeh M, Tahamtan M, et al. Caspase-3: Structure, function, and biotechnological aspects. Biotechnol Appl Biochem. 2022 Aug;69(4):1633–45.

79. Płóciennik A, Prendecki M, Zuba E, Siudzinski M, Dorszewska J. Activated caspase-3 and neurodegeneration and synaptic plasticity in Alzheimer's disease. Adv Alzheimer Dis. 2015;04(03):63–77.

80. Martin LJ. Neuronal death in amyotrophic lateral sclerosis is apoptosis: possible contribution of a programmed cell death mechanism. J Neuropathol Exp Neurol. 1999 May;58(5):459–71.

81. Di Carlo V, Grossi E, Laneve P, Morlando M, Dini Modigliani S, Ballarino M, et al. TDP-43 regulates the microprocessor complex activity during in vitro neuronal differentiation. Mol Neurobiol. 2013 Dec;48(3):952–63.

82. Chou CC, Zhang Y, Umoh ME, Vaughan SW, Lorenzini I, Liu F, et al. TDP-43 pathology disrupts nuclear pore complexes and nucleocytoplasmic transport in ALS/FTD. Nat Neurosci. 2018 Feb;21(2):228–39.

83. Yang C, Tan W, Whittle C, Qiu L, Cao L, Akbarian S, et al. The C-terminal TDP-43 fragments have a high aggregation propensity and harm neurons by a dominant-negative mechanism. PLoS One. 2010 Dec 31;5(12):e15878.

84. Lanznaster D, Hergesheimer R, Vourc'h P, Corcia P, Blasco H. TDP43 aggregates: the "Schrödinger"s cat' in amyotrophic lateral sclerosis. Nat Rev Neurosci. 2021 Aug;22(8):514.

85. Müller M, Jäkel L, Bruinsma IB, Claassen JA, Kuiperij HB, Verbeek MM. MicroRNA-29a Is a Candidate Biomarker for Alzheimer's Disease in Cell-Free Cerebrospinal Fluid. Mol Neurobiol. 2016 Jul;53(5):2894–9.

86. Raheja R, Regev K, Healy BC, Mazzola MA, Beynon V, Von Glehn F, et al. Correlating serum microrna and clinical parameters in amyotrophic lateral sclerosis. Muscle Nerve. 2018 Aug;58(2):261–9.

87. Martí E, Pantano L, Bañez-Coronel M, Llorens F, Miñones-Moyano E, Porta S, et al. A myriad of miRNA variants in control and Huntington's disease brain regions detected by massively parallel sequencing. Nucleic Acids Res. 2010 Nov;38(20):7219–35.

88. Xie H, Zhao Y, Zhou Y, Liu L, Liu Y, Wang D, et al. MiR-9 Regulates the Expression of BACE1 in Dementia Induced by Chronic Brain Hypoperfusion in Rats. Cell Physiol Biochem. 2017 Jul 3;42(3):1213–26.

89. Li Y, Kowdley KV. MicroRNAs in common human diseases. Genomics Proteomics Bioinformatics. 2012 Oct;10(5):246–53.

90. Coppedè F. Epigenetics of neuromuscular disorders. Epigenomics. 2020 Dec;12(23):2125–39.

91. Reichenstein I, Eitan C, Diaz-Garcia S, Haim G, Magen I, Siany A, et al. Human genetics and neuropathology suggest a link between miR-218 and amyotrophic lateral sclerosis pathophysiology. Sci Transl Med [Internet]. 2019 Dec 18;11(523). Available from: http://dx.doi.org/10.1126/scitranslmed.aav5264

92. Amin ND, Bai G, Klug JR, Bonanomi D, Pankratz MT, Gifford WD, et al. Loss of motoneuron-specific microRNA-218 causes systemic neuromuscular failure. Science. 2015 Dec 18;350(6267):1525–9.

93. Jiang ZH, Tang YZ, Song HN, Yang M, Li B, Ni CL. miRNA-342 suppresses renal interstitial fibrosis in diabetic nephropathy by targeting SOX6. Int J Mol Med. 2020 Jan;45(1):45–52.

94. Komoll RM, Hu Q, Olarewaju O, von Döhlen L, Yuan Q, Xie Y, et al. MicroRNA-342-3p is a potent tumour suppressor in hepatocellular carcinoma. J Hepatol. 2021 Jan;74(1):122–34.

95. Junn E, Mouradian MM. MicroRNAs in neurodegenerative diseases and their therapeutic potential. Pharmacol Ther. 2012 Feb;133(2):142–50.

96. Hawley ZCE, Campos-Melo D, Strong MJ. Evidence of A Negative Feedback Network Between TDP-43 and miRNAs Dependent on TDP-43 Nuclear Localization. J Mol Biol. 2020 Dec 4;432(24):166695.

97. Freischmidt A, Müller K, Ludolph AC, Weishaupt JH. Systemic dysregulation of TDP-43 binding microRNAs in amyotrophic lateral sclerosis. Acta Neuropathol Commun. 2013 Jul 30;1:42.

98. Zuo X, Zhou J, Li Y, Wu K, Chen Z, Luo Z, et al. TDP-43 aggregation induced by oxidative stress causes global mitochondrial imbalance in ALS. Nat Struct Mol Biol. 2021 Feb;28(2):132–42.

99. Tufail M, Changxin W. Role of miRNAs in the regulation of cancer-associated signaling pathways. Non-coding RNA Research [Internet]. 2022 Sep 15; Available from: https://www.sciencedirect.com/science/article/pii/S2468054022000518

100. Wang Y, Liu J, Cui J, Sun M, Du W, Chen T, et al. MiR218 Modulates Wnt Signaling in Mouse Cardiac Stem Cells by Promoting Proliferation and Inhibiting Differentiation through a Positive Feedback Loop. Sci Rep. 2016 Feb 10;6:20968.

101. Lu YF, Zhang L, Waye MMY, Fu WM, Zhang JF. MiR-218 mediates tumorigenesis and metastasis: Perspectives and implications. Exp Cell Res. 2015 May 15;334(1):173–82.

102. Ng LF, Kaur P, Bunnag N, Suresh J, Sung ICH, Tan QH, et al. WNT Signaling in Disease. Cells [Internet]. 2019 Aug 3;8(8). Available from: http://dx.doi.org/10.3390/cells8080826

103. Zhang Q, Pan Y, Ji J, Xu Y, Zhang Q, Qin L. Roles and action mechanisms of WNT4 in cell differentiation and human diseases: a review. Cell Death Discov. 2021 Oct 12;7(1):287.

104. Gao Y, Patil S, Qian A. The Role of MicroRNAs in Bone Metabolism and Disease. Int J Mol Sci [Internet]. 2020 Aug 24;21(17). Available from: http://dx.doi.org/10.3390/ijms21176081

105. Hata A, Davis BN. Control of microRNA biogenesis by TGFbeta signaling pathway-A novel role of Smads in the nucleus. Cytokine Growth Factor Rev. 2009 Oct;20(5-6):517–21.

106. Nakamura M, Kaneko S, Ito H, Jiang S, Fujita K, Wate R, et al. Activation of transforming growth factor-β/Smad signaling reduces aggregate formation of mislocalized TAR DNA-binding protein-43. Neurodegener Dis. 2013;11(4):182–93.

107. Pan YB, Zhang CH, Wang SQ, Ai PH, Chen K, Zhu L, et al. Transforming growth factor beta induced (TGFBI) is a potential signature gene for mesenchymal subtype high-grade glioma. J Neurooncol. 2018 Apr;137(2):395–407.

108. Si Y, Cui X, Kim S, Wians R, Sorge R, Oh SJ, et al. Smads as muscle biomarkers in amyotrophic lateral sclerosis. Ann Clin Transl Neurol. 2014 Oct;1(10):778–87.

109. Zhou C, Shen Y, Wei Z, Shen Z, Tang M, Shen Y, et al. ITGA5 is an independent prognostic biomarker and potential therapeutic target for laryngeal squamous cell carcinoma. J Clin Lab Anal. 2022 Feb;36(2):e24228.

110. Zhu H, Wang G, Zhu H, Xu A. ITGA5 is a prognostic biomarker and correlated with immune infiltration in gastrointestinal tumors. BMC Cancer. 2021 Mar 12;21(1):269.

111. Deng Y, Wan Q, Yan W. Integrin α5/ITGA5 Promotes The Proliferation, Migration, Invasion And Progression Of Oral Squamous Carcinoma By Epithelial-Mesenchymal Transition. Cancer Manag Res. 2019 Nov 13;11:9609–20.

112. Gatta V, D'Aurora M, Granzotto A, Stuppia L, Sensi SL. Early and sustained altered expression of aging-related genes in young 3xTg-AD mice. Cell Death Dis. 2014 Feb 13;5:e1054.

113. Büschges R, Weber RG, Actor B, Lichter P, Collins VP, Reifenberger G. Amplification and expression of cyclin D genes (CCND1, CCND2 and CCND3) in human malignant gliomas. Brain Pathol. 1999 Jul;9(3):435–42; discussion 432–3.

114. Kang H, Heo S, Shin JJ, Ji E, Tak H, Ahn S, et al. A miR-194/PTBP1/CCND3 axis regulates tumor growth in human hepatocellular carcinoma. J Pathol. 2019 Nov;249(3):395–408.

115. Liu Z, Wu R, Li G, Sun P, Xu Q, Liu Z. MiR-592 inhibited cell proliferation of human colorectal cancer cells by suppressing of CCND3 expression. Int J Clin Exp Med. 2015 Mar 15;8(3):3490–7.

116. Feng J, Zhou Y, Campbell SL, Le T, Li E, Sweatt JD, et al. Dnmt1 and Dnmt3a maintain DNA methylation and regulate synaptic function in adult forebrain neurons. Nat Neurosci. 2010 Apr;13(4):423–30.

117. Hu T, Chen F, Chen D, Liang H. DNMT3a negatively regulates PTEN to activate the PI3K/AKT pathway to aggravate renal fibrosis. Cell Signal. 2022 Aug;96:110352.

118. Abplanalp WT, Cremer S, John D, Hoffmann J, Schuhmacher B, Merten M, et al. Clonal Hematopoiesis-Driver DNMT3A Mutations Alter Immune Cells in Heart Failure. Circ Res. 2021 Jan 22;128(2):216–28.

119. Zhao JY, Liang L, Gu X, Li Z, Wu S, Sun L, et al. DNA methyltransferase DNMT3a contributes to neuropathic pain by repressing Kcna2 in primary afferent neurons. Nat Commun. 2017 Mar 8;8:14712.

120. Zhou Y, Yang Z, Zhang H, Li H, Zhang M, Wang H, et al. DNMT3A facilitates colorectal cancer progression via regulating DAB2IP mediated MEK/ERK activation. Biochim Biophys Acta Mol Basis Dis. 2022 Apr 1;1868(4):166353.

121. Na F, Pan X, Chen J, Chen X, Wang M, Chi P, et al. KMT2C deficiency promotes small cell lung cancer metastasis through DNMT3A-mediated epigenetic reprogramming. Nat Cancer. 2022 Jun;3(6):753–67.

122. Sanchez-Mut JV, Aso E, Panayotis N, Lott I, Dierssen M, Rabano A, et al. DNA methylation map of mouse and human brain identifies target genes in Alzheimer's disease. Brain. 2013 Oct;136(Pt 10):3018–27.

123. Liu Y, Wang M, Marcora EM, Zhang B, Goate AM. Promoter DNA hypermethylation - Implications for Alzheimer's disease. Neurosci Lett. 2019 Oct 15;711:134403.

124. Zhang HQ, Wang JY, Li ZF, Cui L, Huang SS, Zhu LB, et al. DNA Methyltransferase 1 Is Dysregulated in Parkinson's Disease via Mediation of miR-17. Mol Neurobiol. 2021 Jun;58(6):2620–33.

125. Tie J, Pan Y, Zhao L, Wu K, Liu J, Sun S, et al. MiR-218 inhibits invasion and metastasis of gastric cancer by targeting the Robo1 receptor. PLoS Genet. 2010 Mar 12;6(3):e1000879.

126. Wu DW, Cheng YW, Wang J, Chen CY, Lee H. Paxillin predicts survival and relapse in non-small cell lung cancer by microRNA-218 targeting. Cancer Res. 2010 Dec 15;70(24):10392–401.

127. Mulligan KA, Cheyette BNR. Wnt signaling in vertebrate neural development and function. J Neuroimmune Pharmacol. 2012 Dec;7(4):774–87.

128. Jiang X, Guan Y, Zhao Z, Meng F, Wang X, Gao X, et al. Potential Roles of the WNT Signaling Pathway in Amyotrophic Lateral Sclerosis. Cells [Internet]. 2021 Apr 8;10(4). Available from: http://dx.doi.org/10.3390/cells10040839

129. Libro R, Bramanti P, Mazzon E. The role of the Wnt canonical signaling in neurodegenerative diseases. Life Sci. 2016 Aug 1;158:78–88.

130. Trejo-Solis C, Escamilla-Ramirez A, Jimenez-Farfan D, Castillo-Rodriguez RA, Flores-Najera A, Cruz-Salgado A. Crosstalk of the Wnt/β-Catenin Signaling Pathway in the Induction of Apoptosis on Cancer Cells. Pharmaceuticals [Internet]. 2021 Aug 28;14(9). Available from: http://dx.doi.org/10.3390/ph14090871

131. Shirolkar GD, Pasic S, Gogoi-Tiwari J, Bhat MK, Olynyk JK, Dharmarajan A, et al. Wnt/β-Catenin Signalling during Liver Metabolism, Chronic Liver Disease and Hepatocarcinogenesis. jrenhep. 2018 Mar 15;2(1):1–9.

132. Kahn M. Can we safely target the WNT pathway? Nat Rev Drug Discov. 2014 Jul;13(7):513–32.

133. Ling JP, Pletnikova O, Troncoso JC, Wong PC. TDP-43 repression of nonconserved cryptic exons is compromised in ALS-FTD. Science. 2015 Aug 7;349(6248):650–5.

134. Jeong YH, Ling JP, Lin SZ, Donde AN, Braunstein KE, Majounie E, et al. Tdp-43 cryptic exons are highly variable between cell types. Mol Neurodegener. 2017 Feb 2;12(1):13.

135. Scotter EL, Chen HJ, Shaw CE. TDP-43 Proteinopathy and ALS: Insights into Disease Mechanisms and Therapeutic Targets. Neurotherapeutics. 2015 Apr;12(2):352–63.

136. Brettschneider J, Del Tredici K, Toledo JB, Robinson JL, Irwin DJ, Grossman M, et al. Stages of pTDP-43 pathology in amyotrophic lateral sclerosis. Ann Neurol. 2013 Jul;74(1):20–38.

137. Krus KL, Strickland A, Yamada Y, Devault L, Schmidt RE, Bloom AJ, et al. Loss of Stathmin-2, a hallmark of TDP-43-associated ALS, causes motor neuropathy. Cell Rep. 2022 Jun 28;39(13):111001.

138. Herzog JJ, Deshpande M, Shapiro L, Rodal AA, Paradis S. TDP-43 misexpression causes defects in dendritic growth. Sci Rep. 2017 Nov 15;7(1):15656.

139. Johns AE, Maragakis NJ. Exploring Motor Neuron Diseases Using iPSC Platforms. Stem Cells. 2022 Mar 3;40(1):2–13.